Supporting Information

10-Dibenzothiophenyl-9,9-diphenylacridane Based Multiple Resonance Emitters for High-Efficiency Narrowband Green OLEDs with CIE y > 0.7 at High Doping Concentration.

Rui Zhong, Mengyu Wang, Xingdong Wang, Shumeng Wang, Shiyang Shao*, and Lixiang Wang*

Table of Contents

1. Experimental Details

General information. The chemicals and reagents were obtained from commercial sources (TCI (Shanghai), SigmaAldrich (China) and Energy Chemical (Beijing)) and were used directly. *N, N*-dimethylformamide (DMF) and *tert*-butylbenzene were dried by CaH_2, while tetrahydrofuran (THF)was distilled over sodium/benzophenone before use. $_1H$ and $_{13}C$ NMR spectra were recorded by Bruker Avance NMR spectrometers in $CDCl_3$ and $C_2D_2Cl_4$ with tetramethylsilane (TMS) as the internal standard. Matrix-assisted laser desorption/ionization time of flight (MALDI-TOF) mass spectra were measured on AXIMA CFR MS apparatus (COMPACT). Thermal gravimetric analysis (TGA) was performed on Perkin-Elmer-TGA 7 at heating rate of 10 °C/min with continuous nitrogen flow. Cyclic voltammetry (CV) was carried out in electrochemical workstation (CHI610E) with a typical three-electrode cell (glassy-carbon work electrode, calomel reference electrode and platinum counter electrode) using *n*-Bu_4NClO_4 (0.1 M) as supporting electrolyte and ferrocene as reference at a scan rate of 50 mV s^{-1}. The oxidation and reduction curves were recorded in dichloromethane and DMF (2 mg/mL), respectively. The highest occupied molecular orbital (HOMO) and the lowest unoccupied molecular orbital (LUMO) energy levels of the emitters were calculated according to equations of E_{HOMO}/E_{LUMO} = - (4.80 + $E_{onset}^{ox}/E_{onset}^{red}$), in which E_{onset}^{ox} and E_{onset}^{red} are the onset of oxidation and reduction potentials respectively.

Photophysical measurements. UV-visible absorption was measured by PerkinElmer Lambda 35 UV-vis spectrometer, and photoluminescence (PL) spectra were measured by PerkinElmer LS 50B spectrofluorometer, respectively. PL decay curves were detected on Edinburgh fluorescence spectrometer (FLSP-980). The absolute PLQY values were measured by integrating sphere on Hamamatsu Photonics C9920-2 with excitation wavelength of 345 nm.

Computational method. The calculations were performed with Gaussian 09 package [S1] using density functional theory (DFT) for frontier molecular orbital (FMO) distributions, and time-dependent density functional theory (TD-DFT) for electron excitation transition analysis at the M062x/def2SVP [S2] level. The SOC matrix elements were calculated using the optimized structures by ORCA software package (version

4.1). [S3] The excited states were calculated using SCS-CC2/cc-pVDZ by MRCC software package. [S4-5] Natural transition orbitals (NTO) were performed by Multiwfn (version 3.5) [S6] and drawn by VMD software (version 1.9.3) [S7]. The calculations of RMSD were also completed by VMD software.

Calculation for the Photophysical Parameters. The calculation formulas for the rate constant of radiative decay from S_1 (k_r), non-radiative decay rate constant from S_1 (k_{nr}^s), intersystem crossing (k_{ISC}) and reverse intersystem crossing (k_{RISC}) are expressed as follows [S8]:

$$k_s = 1/\tau_p$$

$$k_d = 1/\tau_d$$

$$k_r = \Phi_p/\tau_p$$
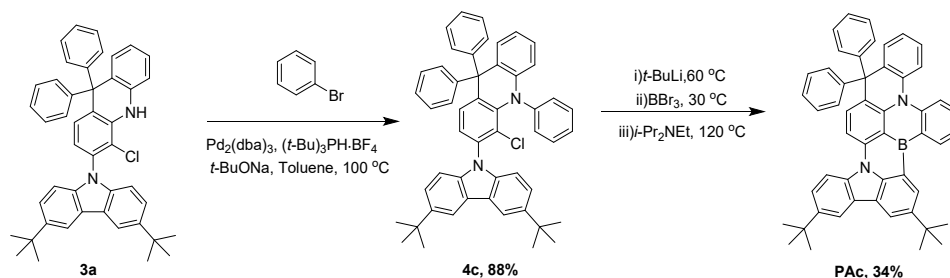
$$\Phi = k_s/(k_s+k_{nr})$$

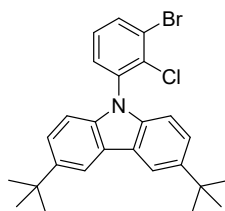$$\Phi_p = k_s/(k_s+k_{nr}+k_{ISC})$$

$$k_{RISC} = k_s k_d/(k_s-k_{ISC})$$

where τ_p and τ_d are the lifetimes of the prompt and delayed components, and Φ and Φ_p are the total and prompt components of the PL quantum efficiency, respectively.

2. Synthetic Procedures

**Scheme S1**. Synthetic routes for control compound **PAc.**

Compound **1**

1

1-Bromo-2-chloro-3-fluorobenzene (32.0 g, 150 mmol), 3,6-bis(*tert*-butyl)-carbazole (46.0 g, 165 mmol) and cesium carbonate (70.0 g, 225 mmol) were mixed in dry DMF (300 mL) under an argon atmosphere. The reaction mixture was stirred at 90 ℃ for 6 hours and then cooled down. The resulting solution was slowly poured into ammonium chloride aqueous solution (1500 mL) and stirred for 30 minutes. Afterward, the precipitate was stirred three times with hot ethanol then dried in a vacuum in 80°C for 5 hours to afford **1** as white powder. Yield: 86 %. ^{1}H NMR (500 Mhz, CDCl$_3$): δ = 8.16 (s, 2H), 7.81 (dd, *J*=8.1, 1.3, 1H), 7.48 − 7.43 (m, 3H), 7.32 (t, *J*=8.0, 1H), 7.00 (d, *J*=8.6, 2H), 1.48 (d, *J*=1.3, 18H). $_{13}$C NMR: (126 MHz, CDCl$_3$) δ = 143.12, 139.09, 137.27, 134.51, 133.56, 129.68, 128.30, 124.51, 123.69, 123.35, 116.36, 109.37, 34.74, 32.00. MALDI-TOF: Calculated: 467.1, Found: 467.1.

Compound **2**
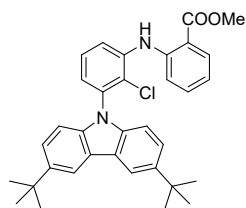
2

Methyl 2-aminobenzoate (18.6 mL, 144 mmol), **1** (56.4 g, 120 mmol,), cesium carbonate (60.0 g, 180 mmol), palladium (II) acetate (0.54 g, 2.4 mmol) and Xantphos (2.80 g, 4.8 mmol) were dissolved in toluene (200 mL) under an argon atmosphere. The reaction mixture was stirred at 100 °C for 12 hours and then cooled down. The reaction mixture was poured into water (200 mL) and extracted with diethyl ether (200 mL). The combined organic layers were dried over sodium sulfate, filtered, and concentrated using a rotary evaporator. The residue was then subjected to column chromatography using dichloromethane/PE (1/10, v/v) as eluent to afford **2** as a faint yellow solid. Yield: 90 %. ^{1}H NMR (500 MHz, CDCl$_3$) δ = 9.82 (s, 1H), 8.16 (s, 2H), 8.05 (dd, J=8.0, 1.2, 1H), 7.69 (dd, J=8.2, 1.0, 1H), 7.52 – 7.43 (m, 4H), 7.37 (t, J=8.0, 1H), 7.14 (dd, J=7.8, 1.1, 1H), 7.09 (d, J=8.6, 2H), 6.95 – 6.88 (m, 1H), 3.94 (s, 3H), 1.48 (s, 18H). ^{13}C NMR (126 MHz, CDCl$_3$) δ = 168.55, 145.62, 142.77, 140.26, 139.29, 137.01, 134.01, 131.87, 127.37, 125.14, 123.76, 123.57, 123.27, 119.45, 119.00, 116.24, 115.35, 114.27, 109.63, 52.07, 34.73, 32.03, 26.91. MALDI-TOF: Calculated: 539.1, Found: 539.1.
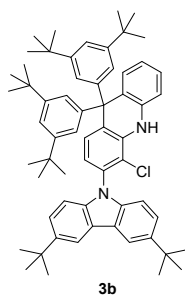
Compound **3a**
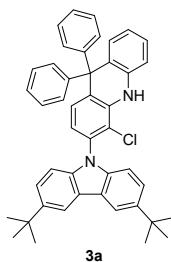
3a

A solution of phenylmagnesium bromide (240 mL, 1 M, 240 mmol) in THF was added dropwise to a solution of **2** (32 g, 60 mmol) in anhydrous THF (150 mL) at 0 °C then stirred at room temperature for 24 hours. After stirring, an ammonium chloride aqueous solution (20 mL) was added dropwise to quench excess phenylmagnesium

bromide. The reaction mixture was poured into water (200 mL) and extracted with diethyl ether (300 mL). The combined organic layers were dried with sodium sulfate, filtered, and concentrated using a rotary evaporator. After the organic solvent was completely removed, the resulting yellow solid was dissolved in THF (150 mL) and added boron trifluoride etherate (74.1 ml, 600 mmol) at room temperature. After stirring for 8 hours, the reaction mixture was poured into water (200 mL) and extracted with diethyl ether (300 mL). The combined organic layers were dried with sodium sulfate, filtered, and concentrated using a rotary evaporator. The residue was then subjected to column chromatography using dichloromethane/PE (1/1, v/v) as eluent to afford **3a** as a faint yellow solid. Yield: 91 %.H NMR (500 MHz, $C_2D_2Cl_4$) δ = 8.07 (d, J=1.7, 2H), 7.39 (dd, J=8.6, 1.8, 2H), 7.29 − 7.19 (m, 7H), 7.07 (s, 1H), 7.02 (d, J=8.6, 2H), 6.98 − 6.88 (m, 8H), 6.82 (d, J=7.4, 1H), 1.40 (s, 18H). ^{13}C NMR (126 MHz, $C_2D_2Cl_4$) δ = 144.89, 142.37, 138.61, 138.00, 137.21, 133.39, 129.97, 129.70, 128.84, 128.37, 127.47, 127.18, 126.95, 126.19, 123.28, 122.41, 121.08, 119.92, 116.70, 115.63, 114.07, 109.36, 34.15, 31.55. MALDI-TOF: Calculated: 644.3, Found: 644.3.

Compound **3b**

3b

A solution of 1-bromo-3,5-di-*tert*-butylbenzene (74.2 mL, 1 M, 74.2 mmol) in THF was added dropwise into a flask with magnesium (1.78 g, 74.2 mmol) and a grain of iodine at room temperature and stirred for 8h to obtain 3,5-di-*tert*-butylphenylmagnesium bromide solution (1M). The aforementioned solution was added dropwise into a solution of **2** (8 g, 14.8 mmol) in anhydrous THF (150 mL) at 0 °C then stirred at room temperature for 24 hours. After stirring, an ammonium chloride aqueous solution (20 mL) was added dropwise to quench excess phenylmagnesium bromide. The reaction mixture was poured into water (100 mL) and extracted with diethyl ether (100 mL).

The combined organic layers were dried with sodium sulfate, filtered, and concentrated using a rotary evaporator. After the organic solvent was completely removed, the resulting yellow solid was dissolved in THF (100 mL) and added boron trifluoride etherate (18.5 ml, 150 mmol) at room temperature. After stirring for 8 hours, the reaction mixture was poured into water (100 mL) and extracted with diethyl ether (100 mL). The combined organic layers were dried with sodium sulfate, filtered, and concentrated using a rotary evaporator. The residue was then subjected to column chromatography using dichloromethane/PE (1/1, v/v) as eluent to afford **3b** as a faint yellow solid. Yield: 89 %.^{1}H NMR (500 MHz, $C_2D_2Cl_4$) δ = 8.05 (d, J=1.0, 2H), 7.35 (dd, J=8.6, 1.5, 2H), 7.17 (m, 3H), 7.02 (s, 1H), 6.98 (d, J=8.6, 2H), 6.96 − 6.84 (m, 5H), 6.66 (d, J=0.9, 4H), 1.39 (s, 18H), 1.12 (s, 36H). ^{13}C NMR (126 MHz, $C_2D_2Cl_4$) δ = 149.04, 144.03, 142.17, 138.75, 137.96, 137.26, 132.86, 129.95, 129.22, 128.82, 127.56, 126.71, 124.12, 123.18, 122.31, 120.67, 119.45, 119.19, 116.34, 115.61, 113.60, 109.26, 34.17, 34.12, 31.55, 30.89. MALDI-TOF: Calculated: 868.5, Found: 868.5.

Compound **4a**

4a
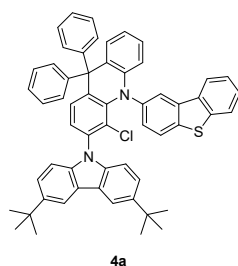
2-Bromodibenzothiophen (4.4 g, 16.8 mmol), **3a** (10.4 g, 16.0 mmol), t-BuONa (2.4 g, 24.0 mmol), Pd$_2$(dba)$_3$ (0.15 g, 0.16 mmol) and t-Bu$_3$PH·BF$_4$ (0.19 g, 0.64 mmol) were dissolved in toluene (50 mL) under an argon atmosphere. The reaction mixture was stirred at 100 °C for 12 hours and then cooled down. The reaction mixture was poured into water (100 mL) and extracted with diethyl ether (100 mL). The combined organic layers were dried with sodium sulfate, filtered, and concentrated using a rotary evaporator. The residue was then subjected to column chromatography using dichloromethane/PE (1/10, v/v) as eluent to afford **4a** as a white solid. Yield: 90 %. ^{1}H NMR (500 MHz, $C_2D_2Cl_4$) δ = 7.97 (d, J=1.6, 2H), 7.72 (dd, J=6.1, 4.2, 2H), 7.69 − 7.64

(m, 1H), 7.49 (d, J=8.6, 1H), 7.39 – 7.33 (m, 2H), 7.33 – 7.29 (m, 1H), 7.25 (dd, J=8.6, 1.8, 2H), 7.23 – 7.10 (m, 9H), 7.08 – 7.03 (m, 1H), 7.00 (d, J=2.0, 1H), 6.93 (d, J=6.8, 4H), 6.89 (d, J=8.6, 2H), 6.73 (dd, J=7.9, 1.3, 1H), 1.32 (s, 18H). ^{13}C NMR (126 MHz, CD$_2$Cl$_2$) δ = 144.83, 143.03, 142.32, 142.23, 142.20, 142.16, 142.05, 142.03, 139.35, 139.32, 138.50, 138.48, 138.02, 135.30, 135.27, 134.91, 134.88, 134.70, 134.37, 134.34, 130.10, 129.80, 128.12, 127.61, 127.00, 126.56, 126.43, 126.39, 126.30, 124.60, 123.68, 123.59, 123.23, 122.47, 122.44, 122.37, 121.67, 121.27, 120.98, 116.41, 115.58, 109.23, 34.11, 31.49. MALDI-TOF: Calculated: 826.3, Found: 826.3.

Compound **4b**

4b
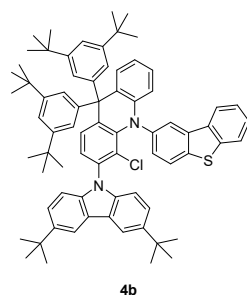
2-Bromodibenzothiophen (3.3 g, 12.1 mmol), **3b** (10.5 g, 12.7 mmol), t-BuONa (1.73 g, 18.0 mmol), Pd$_2$(dba)$_3$ (0.12 g, 0.13 mmol) and t-Bu$_3$PH·BF$_4$ (0.15 g, 0.52 mmol) were dissolved in toluene (50 mL) under an argon atmosphere. The reaction mixture was stirred at 100 °C for 12 hours and then cooled down. The reaction mixture was poured into water (100 mL) and extracted with diethyl ether (100 mL). The combined organic layers were dried with sodium sulfate, filtered, and concentrated using a rotary evaporator. The residue was then subjected to column chromatography using dichloromethane/PE (1/10, v/v) as eluent to afford **4b** as a white solid. Yield: 84 %. ^{1}H NMR (500 MHz, C$_2$D$_2$Cl$_4$) δ = 7.97 (d, J=1.3, 2H), 7.71 – 7.65 (m, 1H), 7.61 (d, J=8.0, 2H), 7.40 (d, J=8.6, 1H), 7.18 (d, J=8.1, 4H), 7.06 (t, J=7.6, 1H), 6.96 (d, J=8.6, 1H), 6.92 (s, 1H), 6.86 (d, J=8.6, 2H), 6.80 (d, J=7.9, 1H), 6.68 (s, 4H), 1.33 (s, 18H), 1.03 (s, 36H). ^{13}C NMR (126 MHz, C$_2$D$_2$Cl$_4$) δ = 149.33, 144.03, 143.04, 142.86, 142.03, 141.91, 141.85, 139.17, 138.72, 138.36, 135.12, 134.70, 134.35, 134.28, 129.67, 127.90, 126.53, 126.14, 126.06, 125.29, 124.66, 123.41, 123.33, 123.13, 122.81, 122.26, 122.22, 121.39, 121.20, 120.35, 119.30, 116.71, 115.56, 109.00, 34.14, 34.06, 31.50, 30.76.

MALDI-TOF: Calculated: 1050.6, Found: 1050.6.

Compound **4c**

4c
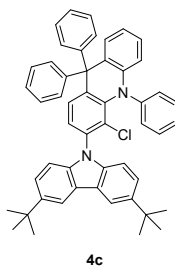
Bromobenzene (2.0 mL, 18.6 mmol), **3a** (10.4 g, 16.0 mmol), t-BuONa (2.4 g, 24.0 mmol), $Pd_2(dba)_3$ (0.15 g, 0.16 mmol) and t-$Bu_3PH\cdot BF_4$ (0.19 g, 0.64 mmol) were dissolved in toluene (50 mL) under an argon atmosphere. The reaction mixture was stirred at 100 °C for 12 hours and then cooled down. The reaction mixture was poured into water (100 mL) and extracted with diethyl ether (100 mL). The combined organic layers were dried with sodium sulfate, filtered, and concentrated using a rotary evaporator. The residue was then subjected to column chromatography using dichloromethane/PE (1/10, v/v) as eluent to afford **4c** as a white solid. Yield: 88 %.^{1}H NMR (500 MHz, $C_2D_2Cl_4$) δ = 8.00 (d, J=1.7, 2H), 7.67 (dd, J=8.1, 0.9, 1H), 7.36 – 7.28 (m, 3H), 7.15 (dd, J=8.5, 5.6, 7H), 7.07 (d, J=8.3, 2H), 6.94 – 6.82 (m, 8H), 6.78 (t, J=7.3, 1H), 6.73 (d, J=1.3, 1H), 6.56 (d, J=7.7, 2H), 1.35 (s, 18H). ^{13}C NMR (126 MHz, $C_2D_2Cl_4$) δ = 144.21, 143.31, 142.60, 142.37, 141.95, 139.53, 138.50, 134.58, 134.54, 134.52, 134.50, 130.00, 129.62, 127.91, 127.75, 127.49, 127.20, 127.19, 126.68, 126.40, 123.83, 123.45, 123.23, 122.58, 122.42, 121.17, 115.62, 109.27, 34.12, 31.52. MALDI-TOF: Calculated: 720.3, Found: 720.3.
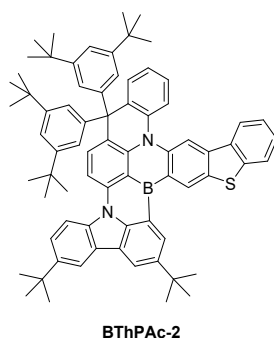
Compound **BThPAc-1**

BThPAc-1
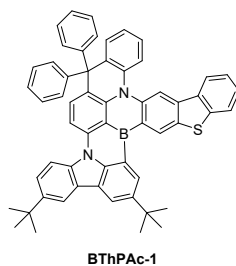
A solution of t-butyllithium in n-hexane (2.4 mL, 1.3 M, 3.0 mmol) was added dropwise into a solution of **4a** (1.0 g, 1.2 mmol) in anhydrous $tert$-butylbenzene (40 mL) at -30

°C under an argon atmosphere. When the addition was finished, the reaction mixture was slowly warmed to 60 °C and stirred for 6 hours. After boron tribromide (0.29 mL, 3.0 mmol) was added at -30 °C, the reaction mixture was slowly warmed to 35 °C and stirred for 3 hours. *N, N*-diisopropylethylamine (0.63 mL, 3.6 mmol) was then added at 0 ºC and the mixture was stirred at 120 ºC for 20 hours. After cooling to room temperature and quenching with water (2 mL), the reaction mixture was concentrated under vacuum at 80 °C. The residue was then subjected to column chromatography using dichloromethane/ PE (1/5, v/v) as eluent. The resulting mixture was recrystallized by *n*-hexane/ethanol for three times to afford **BThPAc-1** as an orange solid. Yield: 55 %. ^{1}H NMR (500 MHz, $C_2D_2Cl_4$) δ = 9.01 (s, 1H), 8.86 (d, *J*=1.6, 1H), 8.46 (d, *J*=1.7, 1H), 8.30 (s, 1H), 8.28 (d, *J*=8.9, 1H), 8.21 (d, *J*=2.0, 1H), 8.18 (d, *J*=8.7, 1H), 7.89 (d, *J*=7.9, 1H), 7.76 (d, *J*=7.9, 1H), 7.68 (d, *J*=8.1, 1H), 7.58 (dd, *J*=8.8, 2.0, 1H), 7.51 (d, *J*=8.6, 1H), 7.49 – 7.10 (m, 10H), 7.07 – 6.95 (m, 3H), 6.73 (s, 2H), 1.62 (s, 9H), 1.45 (s, 9H). ^{13}C NMR (126 MHz, $C_2D_2Cl_4$) δ = 144.97, 144.95, 144.85, 144.60, 142.19, 141.87, 140.99, 140.65, 140.51, 140.21, 137.61, 137.05, 136.17, 134.40, 133.09, 133.04, 129.48, 129.07, 128.57, 128.45, 127.38, 127.33, 127.25, 126.46, 126.19, 126.06, 126.02, 124.66, 124.19, 123.94, 123.32, 123.16, 122.60, 121.91, 120.41, 120.12, 119.62, 119.56, 116.73, 113.62, 112.83, 106.28, 34.67, 34.20, 31.77, 31.31. MALDI-TOF: Calculated: 800.3, Found: 800.3.
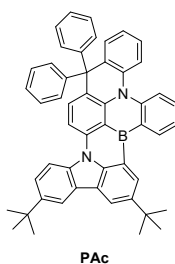
Compound **BThPAc-2**

BThPAc-2

A solution of *t*-butyllithium in *n*-hexane (4.0 mL, 1.3 M, 5.0 mmol) was added dropwise into a solution of **4b** (2.1 g, 2.0 mmol) in anhydrous *tert*-butylbenzene (80 mL) at -30 °C under an argon atmosphere. When the addition was finished, the reaction mixture was slowly warmed to 60 °C and stirred for 6 hours. After boron tribromide (0.48 mL,

5.0 mmol) was added at -30 °C, the reaction mixture was slowly warmed to 35 °C and stirred for 3 hours. *N, N*-diisopropylethylamine (1.05 mL, 6.0 mmol) was then added at 0 °C and the mixture was stirred at 120 °C for 20 hours. After cooling to room temperature and quenching with water (2 mL), the reaction mixture was concentrated under vacuum at 80 °C. The residue was then subjected to column chromatography using dichloromethane/ PE (1/5, v/v) as eluent. The resulting mixture was recrystallized by *n*-hexane/ethanol for three times to afford **BThPAc-2** as an orange solid. Yield: 45 %. ^{1}H NMR (500 MHz, $C_2D_2Cl_4$) δ = 9.04 (s, 1H), 8.91 (s, 1H), 8.49 (d, *J*=1.5, 1H), 8.42 (s, 1H), 8.39 (d, *J*=8.9, 1H), 8.25 (s, 2H), 7.88 (d, *J*=7.6, 1H), 7.81 – 7.69 (m, 3H), 7.63 (d, *J*=8.7, 1H), 7.44 – 7.31 (m, 4H), 7.22 (t, *J*=7.5, 1H), 7.15 (t, *J*=7.4, 1H), 7.01 – 6.91 (m, 3H), 6.60 (s, 1H), 6.47 (s, 1H), 1.65 (s, 9H), 1.48 (s, 9H), 1.26 (s, 9H), 1.20 (s, 9H), 1.17 (s, 9H), 0.85 (s, 9H). ^{13}C NMR (126 MHz, $C_2D_2Cl_4$) δ = 148.97, 148.84, 148.72, 148.62, 148.59, 144.79, 144.51, 144.41, 143.38, 142.26, 142.12, 140.97, 140.46, 140.42, 139.86, 137.63, 137.06, 134.50, 132.88, 132.55, 129.46, 128.85, 128.59, 127.35, 126.30, 126.16, 125.95, 125.77, 125.60, 124.01, 123.96, 123.20, 122.99, 122.68, 122.44, 121.61, 120.22, 119.59, 119.11, 118.60, 116.75, 113.68, 113.12, 105.84, 73.63, 73.59, 73.37, 73.15, 34.64, 34.29, 34.21, 34.18, 31.77, 31.32, 31.03, 30.89, 30.64. MALDI-TOF: Calculated: 1024.6, Found: 1024.6.

Compound **PAc**

PAc

A solution of *t*-butyllithium in *n*-hexane (4.0 mL, 1.3 M, 5.0 mmol) was added dropwise into a solution of **4c** (1.4 g, 2.0 mmol) in anhydrous *tert*-butylbenzene (80 mL) at -30 °C under an argon atmosphere. When the addition was finished, the reaction mixture was slowly warmed to 60 °C and stirred for 6 hours. After boron tribromide (0.48 mL, 5.0 mmol) was added at -30 °C, the reaction mixture was slowly warmed to 35 °C and stirred for 3 hours. *N, N*-diisopropylethylamine (1.05 mL, 6.0 mmol) was then added

at 0 ºC and the mixture was stirred at 120 ºC for 20 hours. After cooling to room temperature and quenching with water (2 mL), the reaction mixture was concentrated under vacuum at 80 ºC. The residue was then subjected to column chromatography using dichloromethane/ PE (1/5, v/v) as eluent. The resulting mixture was recrystallized by n-hexane/ethanol for three times to afford **PAc** as a yellow solid. Yield: 34 %. ^{1}H NMR (500 MHz, $C_2D_2Cl_4$) δ = 8.81 (d, J=1.7, 1H), 8.63 (dd, J=7.6, 1.2, 1H), 8.40 (d, J=1.7, 1H), 8.25 (d, J=8.9, 1H), 8.17 (d, J=2.0, 1H), 8.13 (d, J=8.7, 1H), 7.65 (d, J=8.4, 1H), 7.59 – 7.53 (m, 2H), 7.49 (d, J=8.6, 1H), 7.45 – 6.59 (m, 15H), 1.56 (s, 9H), 1.43 (s, 9H). ^{13}C NMR (126 MHz, $C_2D_2Cl_4$) δ = 144.92, 144.84, 144.73, 144.51, 144.36, 141.99, 140.95, 140.18, 140.04, 137.54, 136.02, 135.07, 132.85, 129.97, 129.35, 128.94, 128.36, 127.26, 127.20, 126.39, 126.12, 125.88, 125.80, 124.63, 124.08, 123.30, 122.92, 122.21, 120.53, 120.26, 120.08, 119.93, 119.76, 116.64, 113.54, 106.16, .59, 34.17, 31.72, 31.29. MALDI-TOF: Calculated: 733.4, Found: 733.4.

3. Crystallographic Data Collection and Structure Determination

Table S1. Crystal data and structure refinement of **BThPAc-1**. (CCDC number: 2350022).

Identification code	BNNS
Empirical formula	$C_{60}H_{52}BN_2S$
Formula weight	843.9
Temperature/K	300
Crystal system	triclinic
Space group	P-1
a/Å	11.287(6)
b/Å	12.693(6)
c/Å	18.454(10)
α/°	101.306(14)
β/°	101.726(15)
γ/°	97.471(14)
Volume/Å^3	2499(2)
Z	2
ρ_{calc}g/cm^3	1.122
μ/mm^{-1}	0.104
F(000)	894
Crystal size/mm^3	0.2 × 0.2 × 0.1
Radiation	MoKα (λ = 0.71073)
2Θ range for data collection/°	3.912 to 60.784
Index ranges	-16 ≤ h ≤ 15, -17 ≤ k ≤ 17, -26 ≤ l ≤ 26
Reflections collected	139869
Independent reflections	14837 [R_{int} = 0.1410, R_{sigma} = 0.0918]
Data/restraints/parameters	14837/46/612
Goodness-of-fit on F^2	1.066
Final R indexes [I>=2σ (I)]	R_1 = 0.0976, wR_2 = 0.2474
Final R indexes [all data]	R_1 = 0.1857, wR_2 = 0.3020
Largest diff. peak/hole / e Å^{-3}	0.92/-0.41

4. DFT calculation
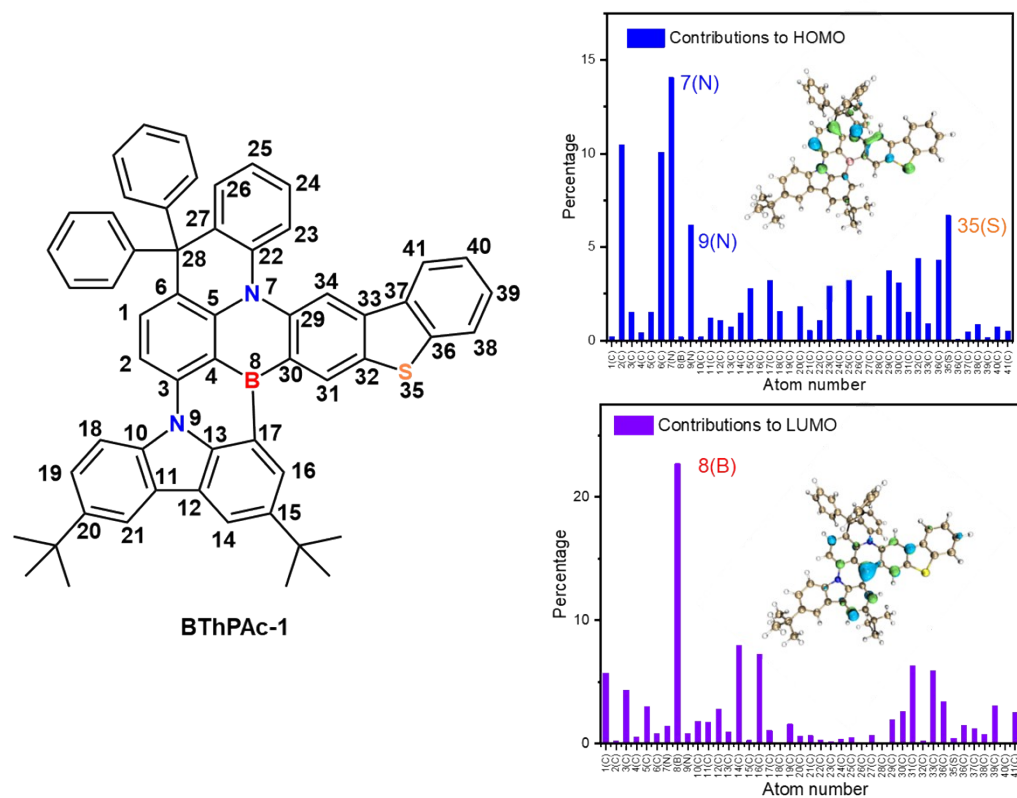
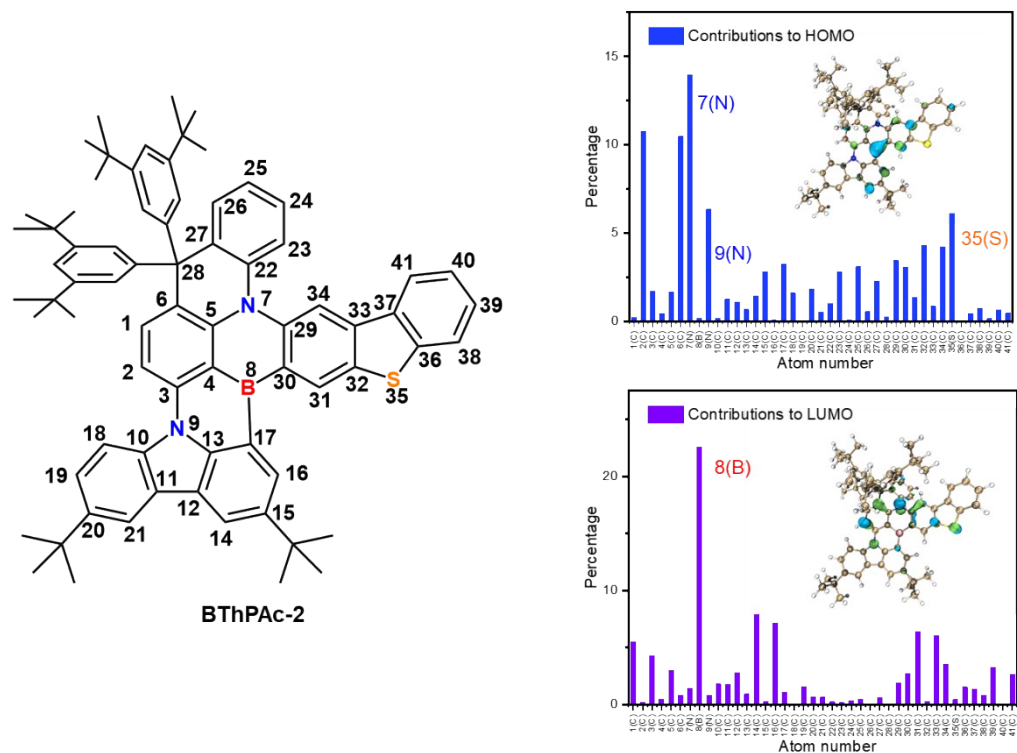**Figure S1.** Mulliken analysis for **BThPAc-1** by Multiwfn software package.

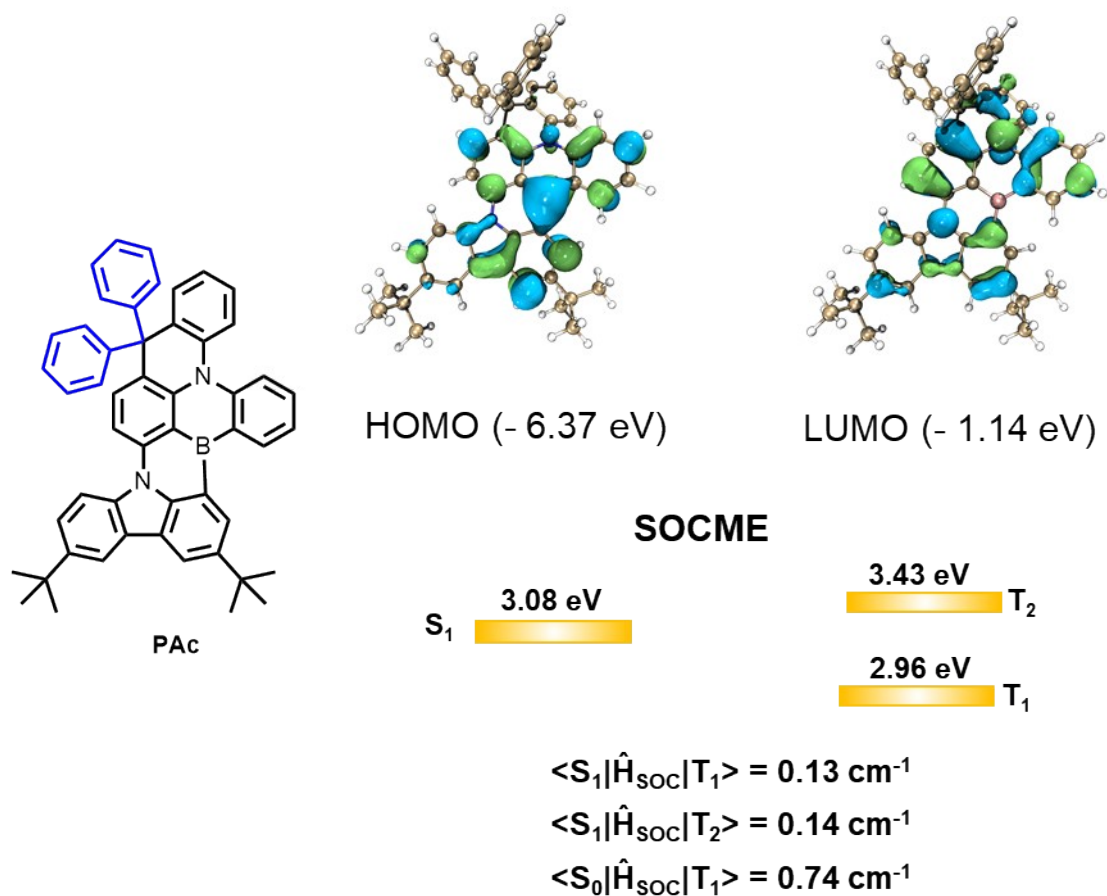**Figure S2.** Mulliken analysis for **BThPAc-2** by Multiwfn software package.

HOMO (- 6.37 eV)   LUMO (- 1.14 eV)

SOCME

S_1 3.08 eV

T_2 3.43 eV

T_1 2.96 eV

$\langle S_1|\hat{H}_{SOC}|T_1\rangle = 0.13$ cm^{-1}

$\langle S_1|\hat{H}_{SOC}|T_2\rangle = 0.14$ cm^{-1}

$\langle S_0|\hat{H}_{SOC}|T_1\rangle = 0.74$ cm^{-1}

Figure S3. HOMO/LUMO distributions and SOCME values for **PAc**.
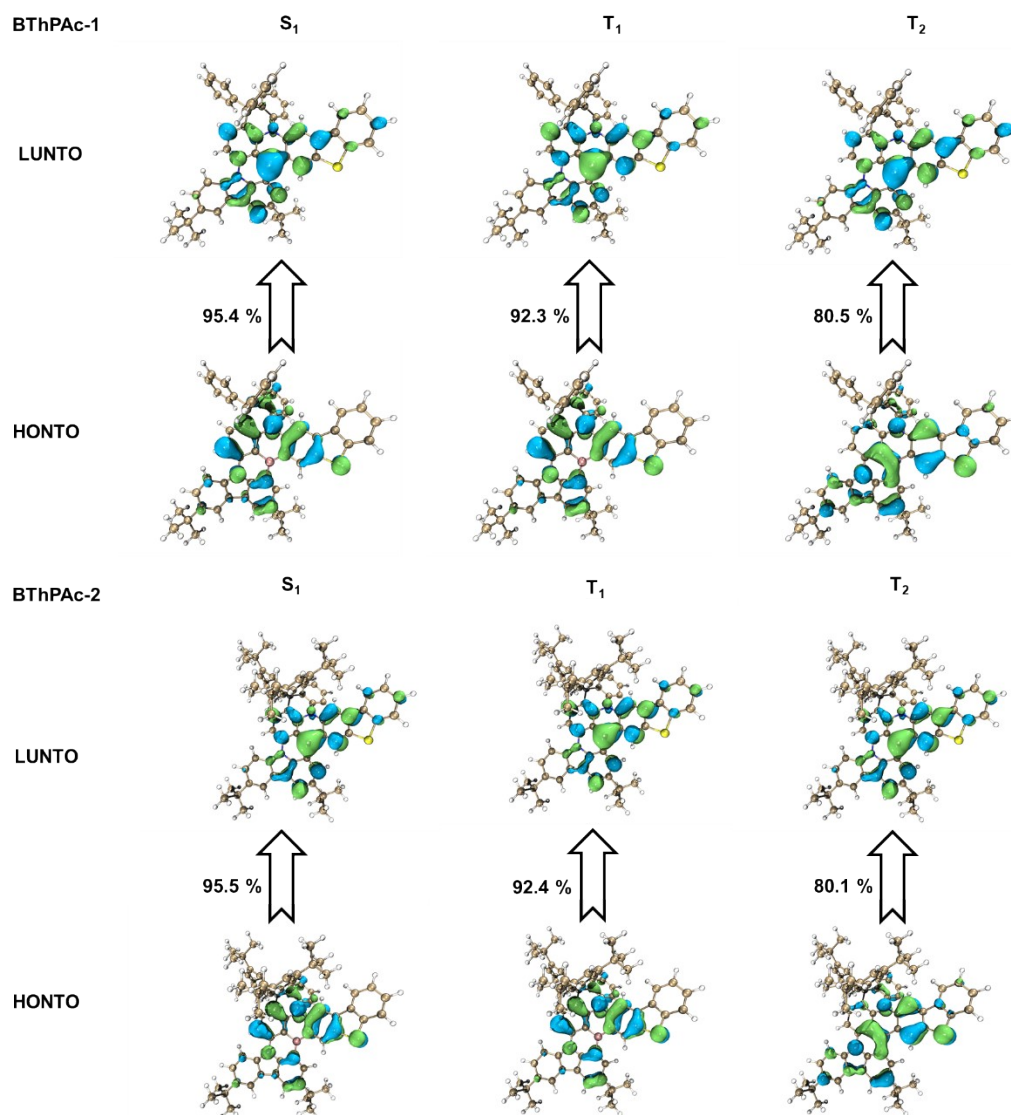
Figure S4. Natural transition orbitals (NTOs) for **BThPAc-1** and **BThPAc-2**.

Table S2. Summary of TD-DFT calculation results for the emitters.

Compound	Optimized structure	Transition	Wavelength [nm]	Energy [eV]	Oscillator strength	Electron configurations
BThPAc-1	S_0	$S_0\text{-}S_1$	387.44	3.2001	0.4250	H -> L 93.2%
		$S_0\text{-}T_1$	451.75	2.7445	0.0000	H -> L 87.1% H-1 -> L+1 2.4%
	S_1	$S_1\text{-}S_0$	414.09	3.0425	0.3786	H -> L 94.2%
	T_1	$T_1\text{-}S_0$	486.17	2.5502	0.0000	H -> L 88.7% H-1 -> L+1 2.1%
BThPAc-2	S_0	$S_0\text{-}S_1$	390.08	3.1784	0.4112	H -> L 93.6%
		$S_0\text{-}T_1$	454.59	2.7274	0.0000	H -> L 88.2% H-1 -> L+1 2.4%
	S_1	$S_1\text{-}S_0$	409.75	3.0259	0.3686	H -> L 94.3%
	T_1	$T_1\text{-}S_0$	487.89	2.5412	0.0000	H -> L 88.4% H-1 > L+1 2.1%
PAc	S_0	$S_0\text{-}S_1$	371.01	3.3418	0.4654	H -> L 94.2%
		$S_0\text{-}T_1$	434.20	2.8554	0.0000	H -> L 88.7%
	S_1	$S_1\text{-}S_0$	387.05	3.2033	0.4353	H -> L 94.5%
	T_1	$T_1\text{-}S_0$	456.35	2.7169	0.0000	H -> L 88.7%

5. Thermal characteristics
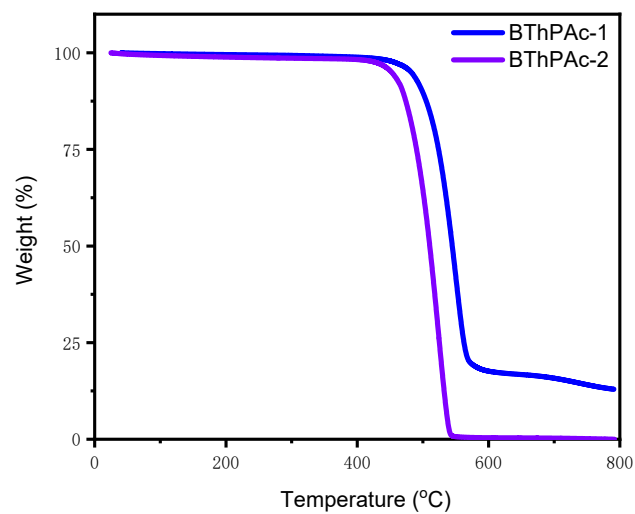
Figure S5. Thermogravimetric analysis (TGA) curves for **BThPAc-1** and **BThPAc-2**.

6. Electrochemical measurements
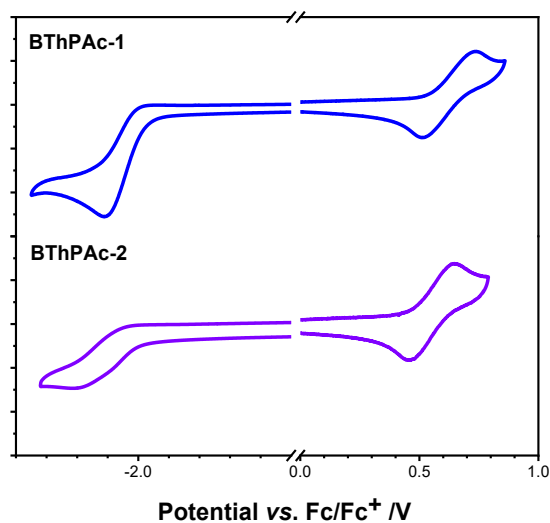
Figure S6. Cyclic voltammetry (CV) characteristics for **BThPAc-1** and **BThPAc-2**
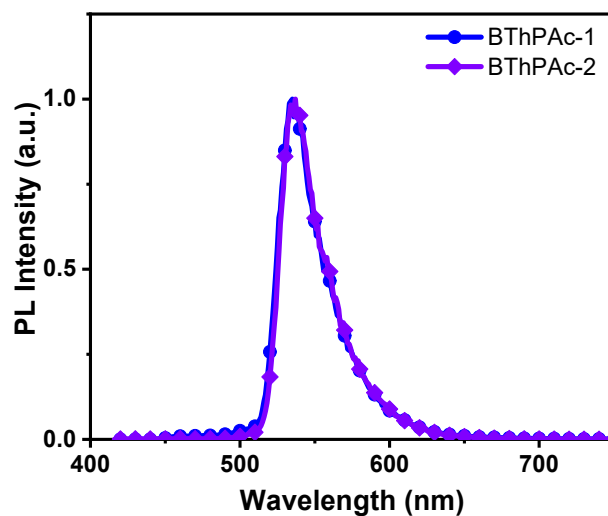
7. Photophysical properties

Figure S7. Low-temperature phosphorescence spectra (77 K) of **BThPAc-1** and **BThPAc-2** in toluene with concentration of 10^{-5} mol L^{-1}.
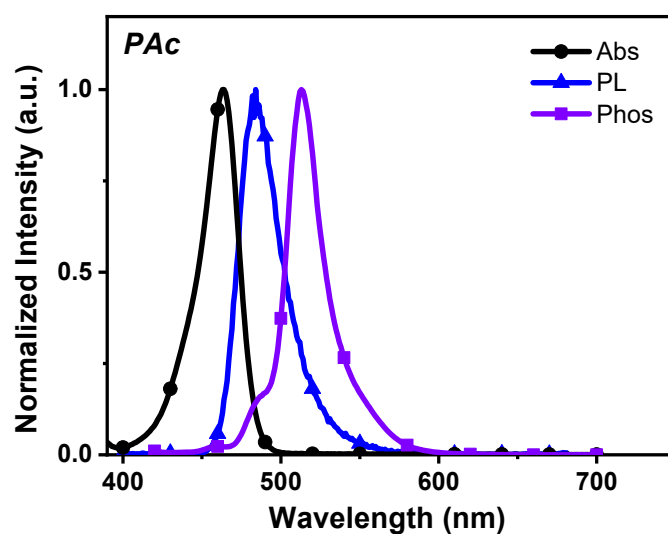

Figure S8. UV-visible absorption (Abs), fluorescence (PL) and phosphorescence (Phos, 77 K) spectra of **PAc** in toluene with concentration of 10^{-5} mol L^{-1}.

Table S3. Summary of photophysical properties for **PAc**.

| | λ_{abs}[a)] | λ_{em}[b)] | FWHM[c)] | Φ_{PLQY}[d)] | τ_p/τ_d[e)] | k_r[f)] | k_{ISC}[f)] | k_{RISC}[f)] | S_1/T_1[g)] | ΔE_{ST}[h)] |
	[nm]	[nm]	[nm]		[ns/μs]	[10^7 S^{-1}]	[10^7 S^{-1}]	[10^5 S^{-1}]	[eV]	[eV]
PAc	464	484	30	0.83	6.5/17.7	12.0	1.5	0.6	2.68 /2.52	0.16

[a)] Absorption peak measured in toluene solution (10^{-5} M). [b)] Emission peak measured in toluene solution (10^{-5} M). [c)] Full width at half maximum of the PL spectrum. [d)] Photoluminescence quantum yield measured in doping films in mCP (5 wt%). [e)] Prompt and delayed fluorescence lifetimes of doping films. [f)] k_r, k_{ISC} and k_{RISC} represents the rate constant of radiative decay of S_1, intersystem crossing from S_1 to T_1 and reverse intersystem crossing from T_1 to S_1. [g)] Singlet (S_1) and triplet (T_1) state energy levels estimated from fluorescence peak and phosphorescence spectra. [h)] Energy gap between S_1 and T_1.
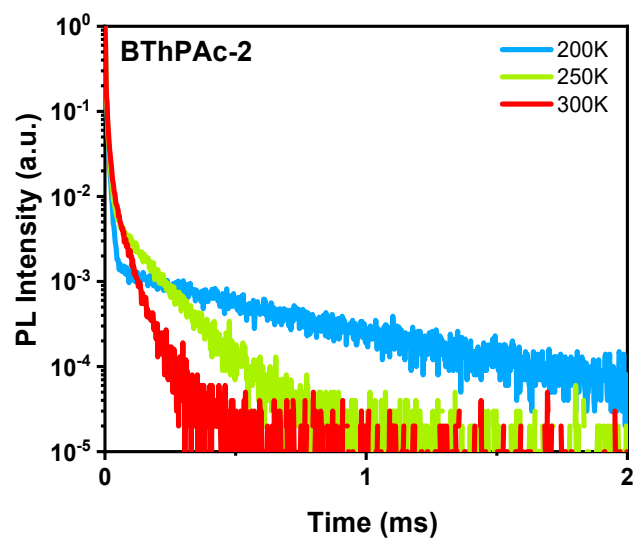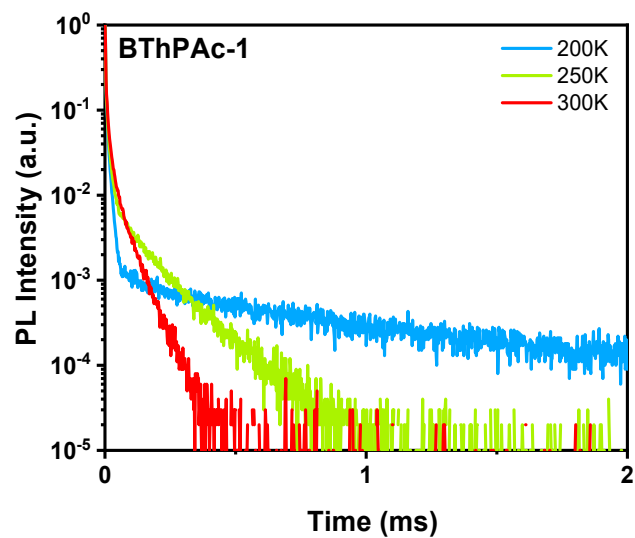
Figure S9. Transient PL decay spectra for **BThPAc-1** and **BThPAc-2** in film (1 wt % doped in mCP) at 150–300 K.
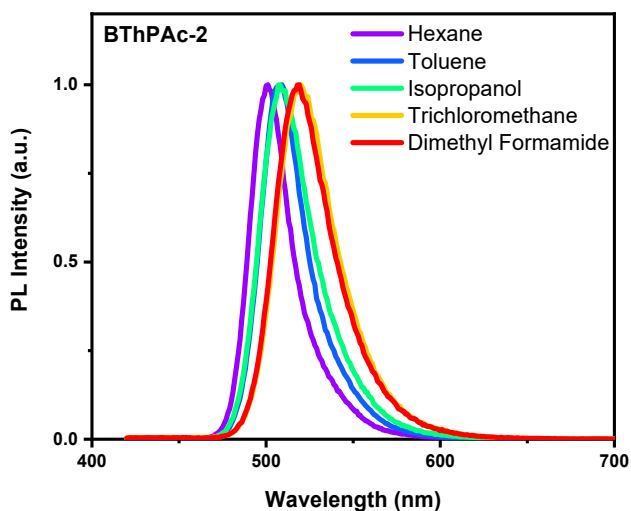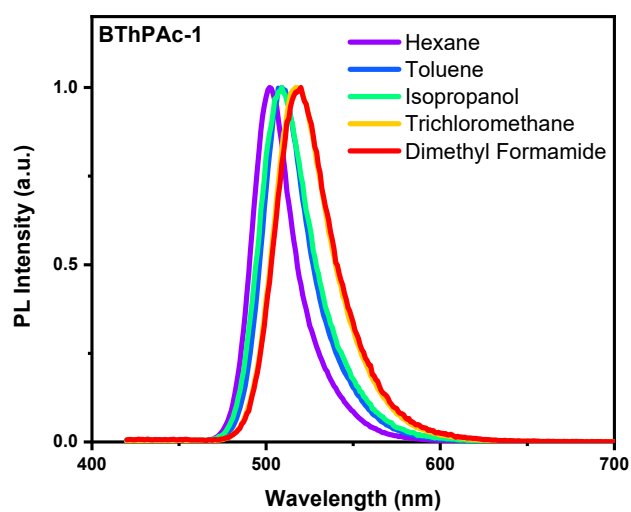
Figure S10. PL spectra for **BThPAc-1** and **BThPAc-2** in solvents with different polarity.

Table S4. Emission peak and FWHM for **BThPAc-1** and **BThPAc-2** in solvents with different polarity.

	λ_{em}/FWHM [nm]				
Compound	Hexane	Toluene	Isopropanol	Trichloromethane	Dimethyl Formamide
BThPAc-1	502 / 27	509 / 30	509 / 34	517 / 36	520 / 37
BThPAc-2	501 / 27	509 / 30	508 / 35	520 / 38	519 / 38
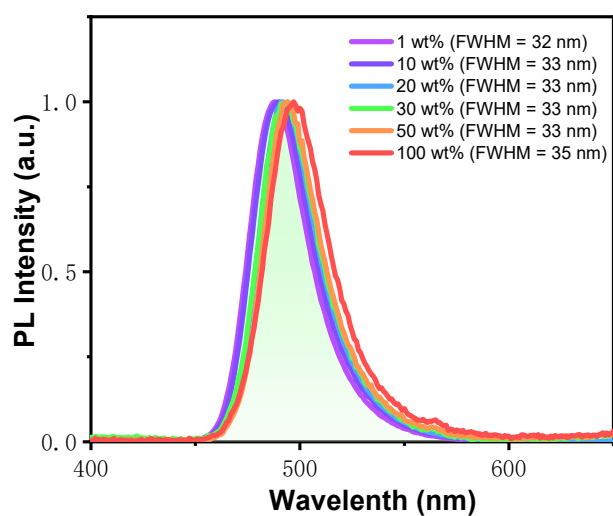
Figure S11. PL spectra for doped films **of PAc** in mCP with different dopant concentrations.

Table S5. Summary of emission spectra of doped films with different dopant concentrations in mCP (mCP: x wt% for **BThPAc-1**, **BThPAc-2** and **PAc)**.

	λ_{em} / FWHM [nm]					
	1%	10%	20%	30%	50%	100%
BThPAc-1	509/32	509/32	511/34	515/34	514/34	520/35
BThPAc-2	510/32	511/32	511/32	513/33	513/33	515/34
PAc	488/32	490/33	492/33	494/33	494/33	497/35

8. OLED device performance
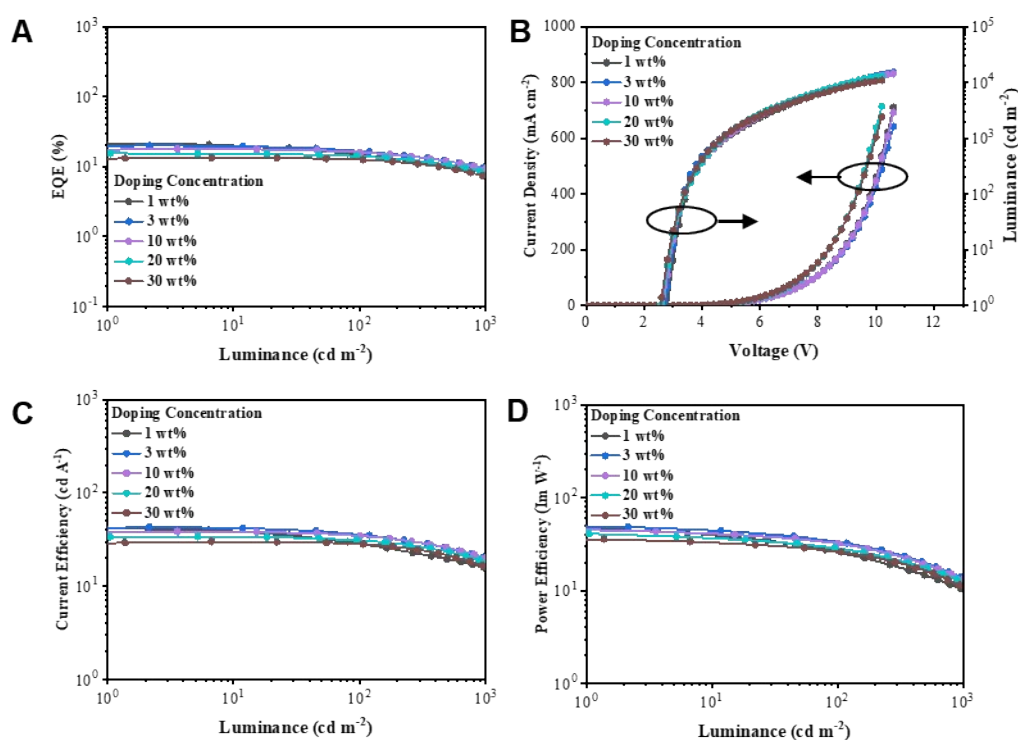
Figure S12. EQE-*L* curves (A), *J-V-L* curves (B), CE-*L* curves (C) and PE-*L* curves (D) for **PAc**-based OLEDs.

Table S6. Summary of OLED device performance for **PAc**.

	Doping Concentration	V_{on}[a] [V]	L_{max}[b] [cd/m^2]	CE_{max}[c] [cd/A]	PE_{max}[d] [lm/W]	$EQE_{Max/100/1000}$[e] [%]	FWHM[f] [nm]	λ_{EL}[g] [nm]	CIE[h] (x, y)
	1 wt%	2.80	14308	40.2	42.0	20.7/15.1/8.3	33.4	489	0.093, 0.399
	3 wt%	2.68	15344	43.2	48.5	20.1/16.9/9.5	34.9	492	0.096, 0.469
PAc	10 wt%	2.63	14297	38.4	43.1	17.7/16.1/9.4	34.3	494	0.097, 0.480
	20 wt%	2.59	12741	34.0	40.9	15.5/14.1/8.3	34.7	494	0.099, 0.494
	30 wt%	2.54	10864	30.1	35.6	13.3/12.6/7.2	35.0	495	0.102, 0.505

[a] Turn-on voltage at luminance of 1 cd m^{-2}. [b] Maximum luminance. [c] Maximum luminous efficiency. [d] Maximum power efficiency [e] External quantum efficiency at maximum and at luminance of 100/1000 cd m^{-2}. [f] Full-width at half-maximum at 1000 cd/m^2. [g] EL maximum at 1000 cd m^{-2}. [h] CIE coordinates at 1000 cd m^{-2}.

Table.S7 Comparison for OLED performance of **BThPAc-1**, **BThPAc-2** and reported MR-TADF emitters with high doping concentrations (> 15 wt%).

Emitter	Doping Condition	EQE$_{Max/100/1000}$[a]	λ$_{EL}$[b] [nm]	FWHM[c] [nm]	CIE[d] (x, y)	Ref.
BThPAc-1	3 wt%	24.8/22.8/15.5	516	34	0.17, 0.72	This work
	30 wt%	17.0/16.9/12.9	518	34	0.19, 0.72	
BThPAc-2	3 wt%	26.5/22.0/14.4	514	33	0.16, 0.71	This work
	30 wt%	20.3/20.0/14.6	517	33	0.18, 0.72	
D-Cz-BN	1 wt%	37.2/37.2/34.3	488	24	0.11, 0.43	S9
	20 wt%	36.3/36.2/25.8	491	24	0.10, 0.41	
S-Cz-BN	1 wt%	30.5/30.2/26.2	488	26	0.12, 0.43	S9
	20 wt%	28.8/26.9/18.9	494	31	0.10, 0.46	
BN-CP1	5 wt%	40.0/34.0/18.5	496	25	0.09, 0.50	S10
	30 wt%	33.3/24.2/12.8	496	25	0.08, 0.52	
BN-CP2	5 wt%	36.4/32.6/19.2	497	26	0.10, 0.53	S10
	30 wt%	23.7/20.3/9.8	502	33	0.16, 0.62	
M-Cz-BNCz	3 wt%	27.0/24.2/14.4	520	44	0.23, 0.69	S11
	30 wt%	27.3/25.4/15.7	528	47	0.28, 0.67	
*p*BP-DABNA-Me	5 wt%	23.4/-/-	464	23	0.13, 0.09	S12
	20 wt%	20.6/-/-	464	23	0.13, 0.09	
tCBNDADPO	-	-	-	-	-	S13
	30 wt%	30.8/23.3/16.2	472	28	0.14, 0.22	
DPMX-CzDABNA	5 wt%	24.5/15.5/8.2	484	29	0.11, 0.31	S14
	20 wt%	26.8/20.7/7.9	484	29	0.11, 0.33	
TCzBN-oPh	1 wt%	26.0/22.9/10.4	492	28	0.09, 0.46	S15
	20 wt%	24.2/14.7/3.7	496	31	0.11, 0.54	
TCzBN-DPF	1 wt%	24.8/19.1/11.3	496	28	0.09, 0.53	S15
	20 wt%	24.2/19.2/9.2	501	36	0.17, 0.60	
TCzBN-TMPh	1 wt%	25.1/18.4/6.5	488	27	0.11, 0.38	S15
	20 wt%	18.6/6.9/0.8	488	27	0.10, 0.39	

D-m-1PCzBN	2 wt%	32.6/29.5/22.3	500	30	0.10, 0.56	S16
	30 wt%	25.6/19.3/13.3	508	34	0.16, 0.65	
D-p-1PCzBN	2 wt%	33.5/26.4/16.5	495	26	0.07, 0.50	S16
	30 wt%	28.5/22.6/10.0	498	27	0.10, 0.55	
BSS-Ph-TBCz	5 wt%	21.4/-/-	468	31	0.12,0.11	S17
	25 wt%	20.1/-/-	470	31	0.12,0.12	
4FlCzBN	2 wt%	10.1/5.6/4.0	497	28	0.09, 0.53	S18
	16 wt%	10.9/6.7/4.6	500	30	0.11, 0.57	

[a] Maximum EQE and EQE at a luminance of 100/1000 cd m^{-2}. [b] EL emission maximum. [c] Full-width at half-maximum for EL emission. [d] CIE coordinates.

9. Appendix: NMR and mass spectra
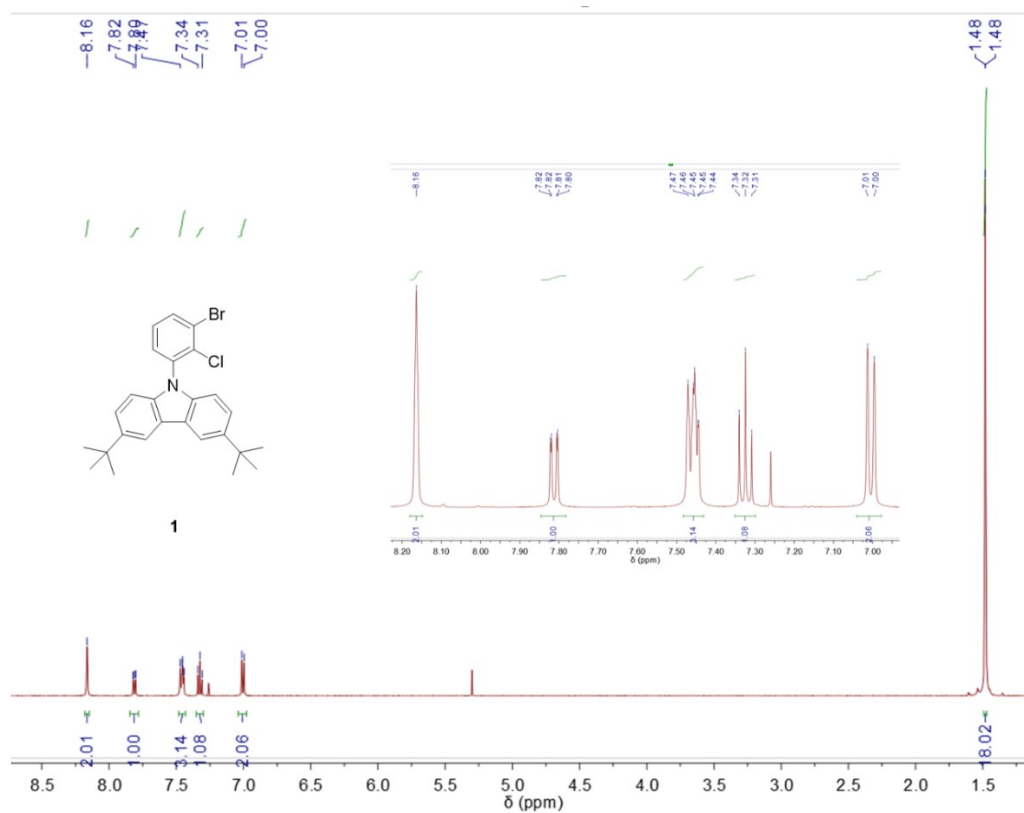
Figure S13. ^{1}H NMR spectra of **1**.
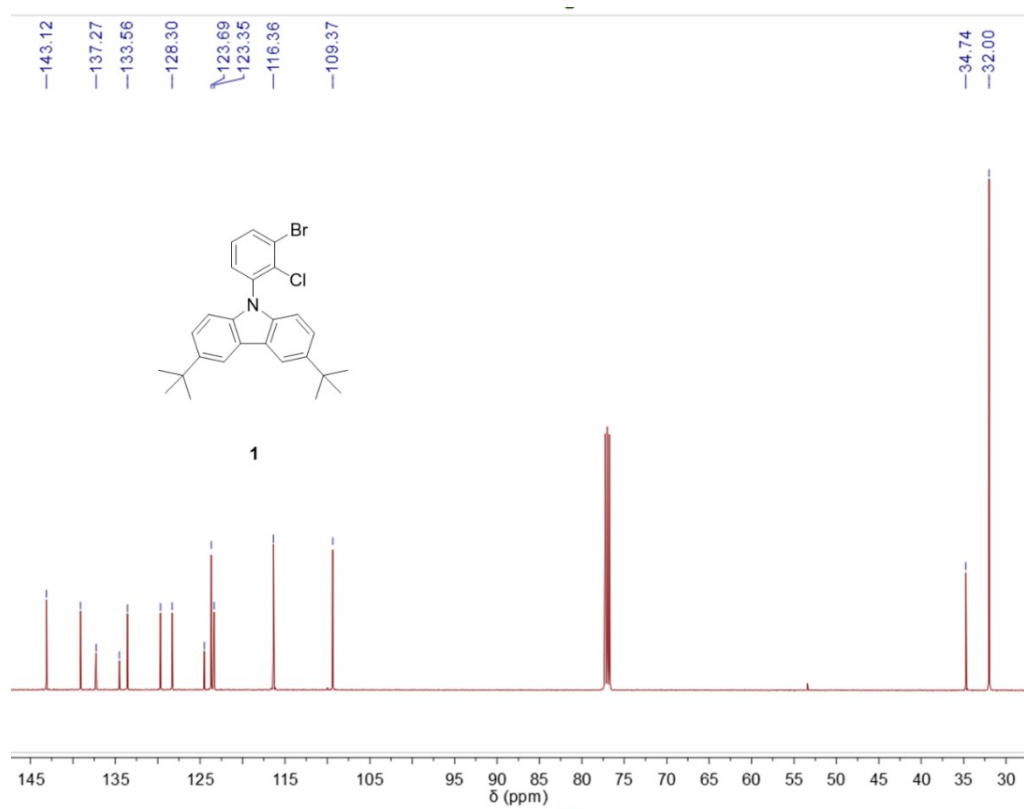
Figure S14. ^{13}C NMR spectra of **1**.
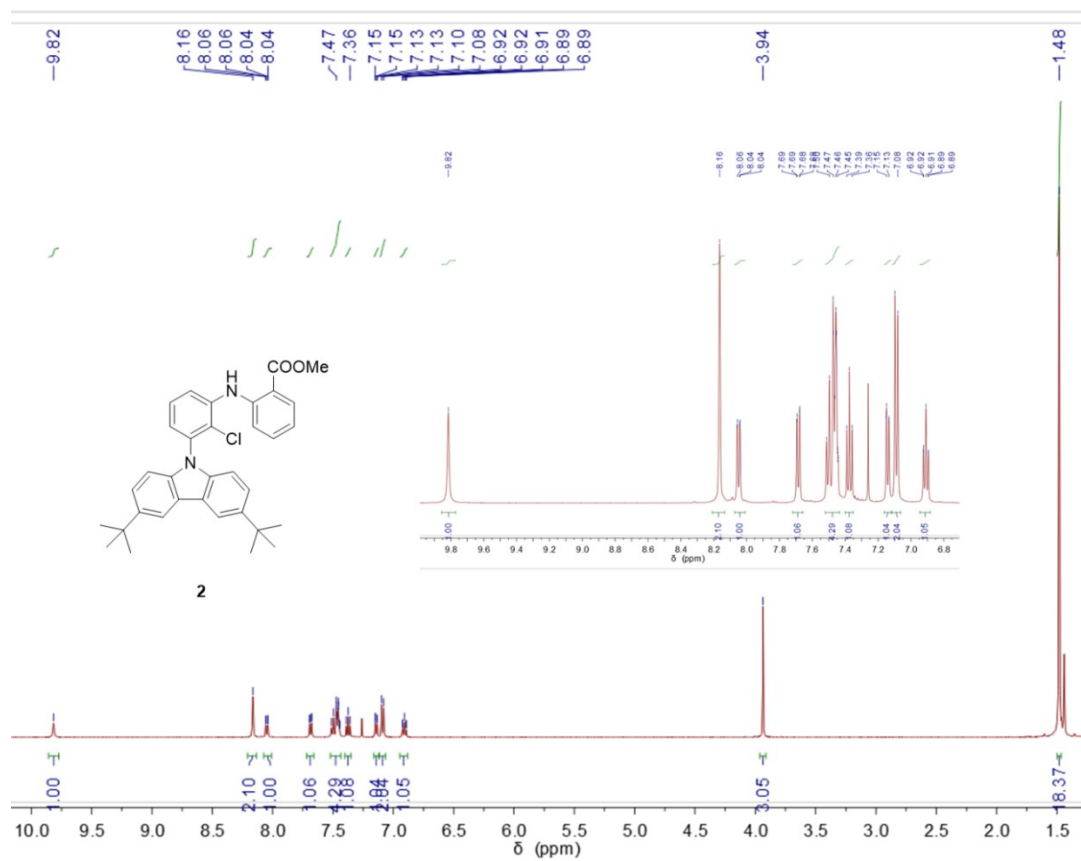
Figure S15. ^{1}H NMR spectra of **2**.
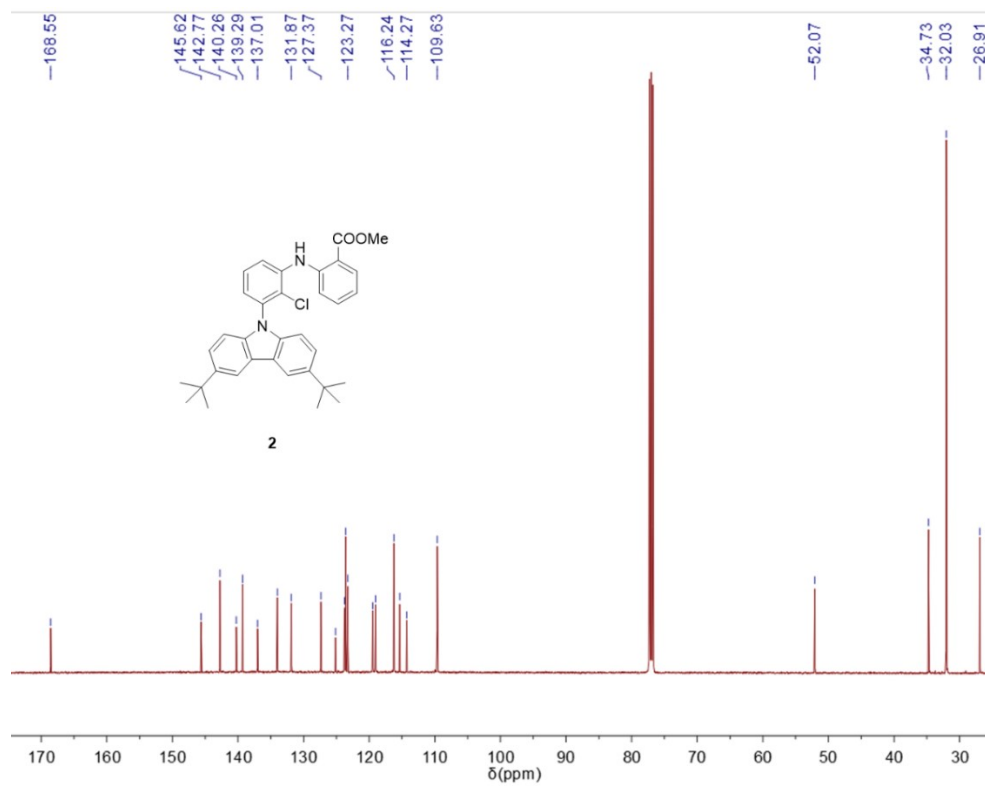
Figure S16. ^{13}C NMR spectra of **2**.
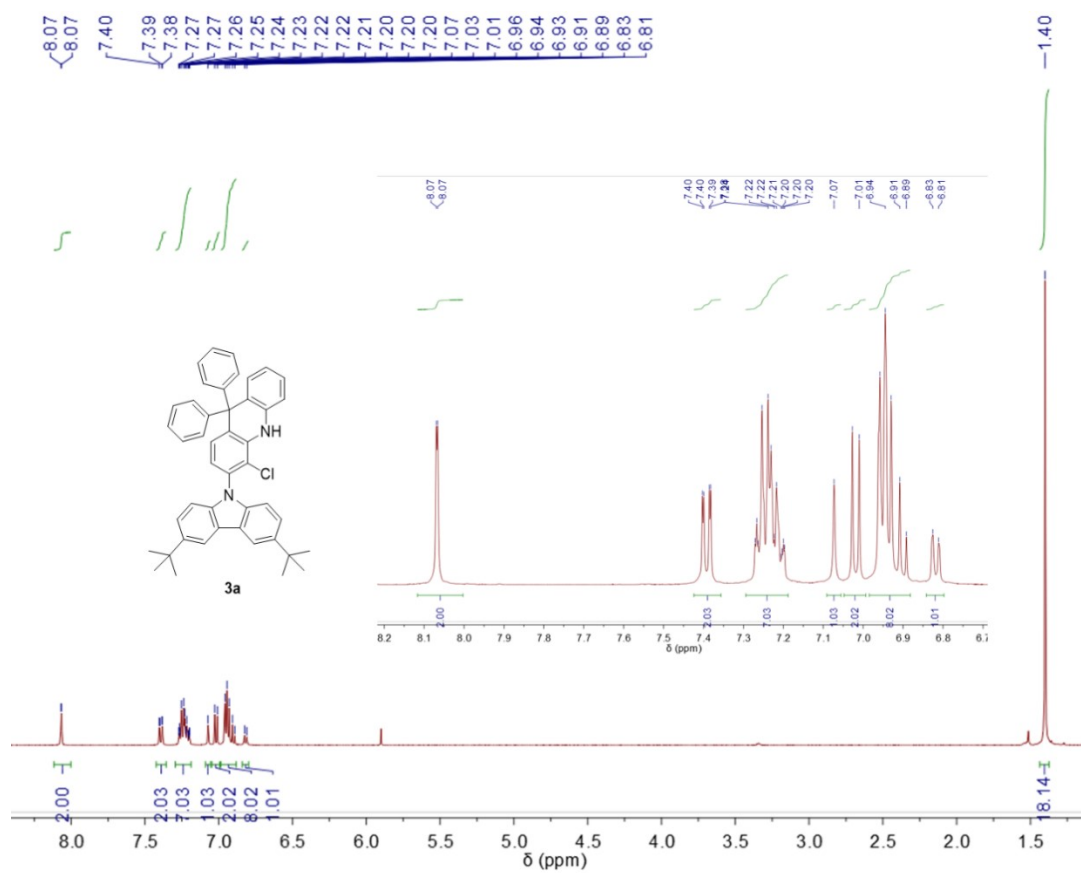
Figure S17. ^{1}H NMR spectra of **3a.**
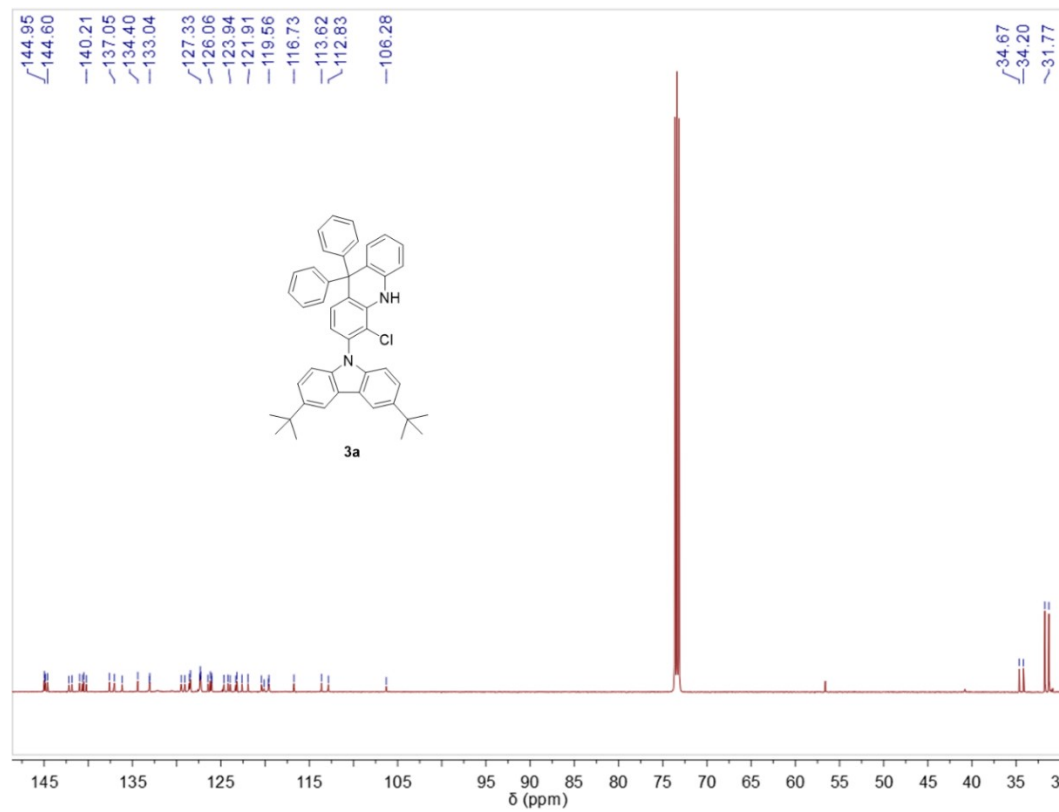
Figure S18. ^{13}C NMR spectra of **3a.**
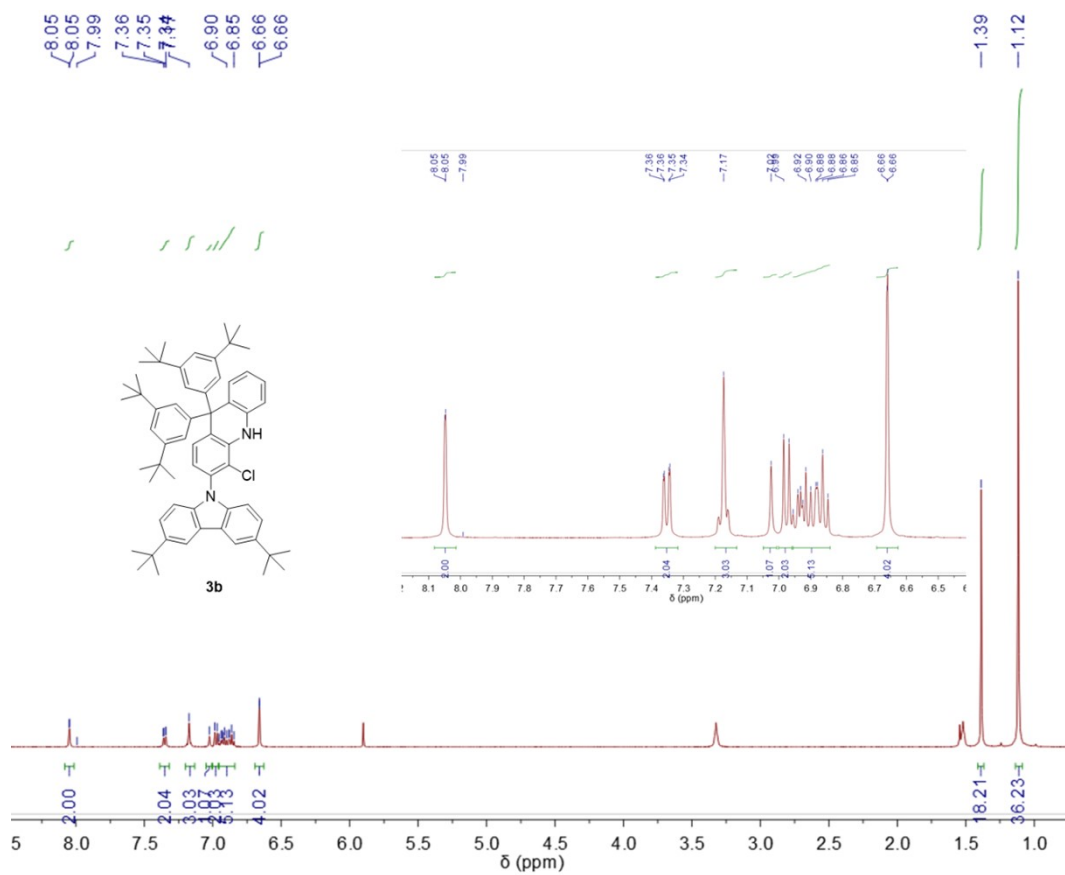
Figure S19. ^{1}H NMR spectra of **3b.**
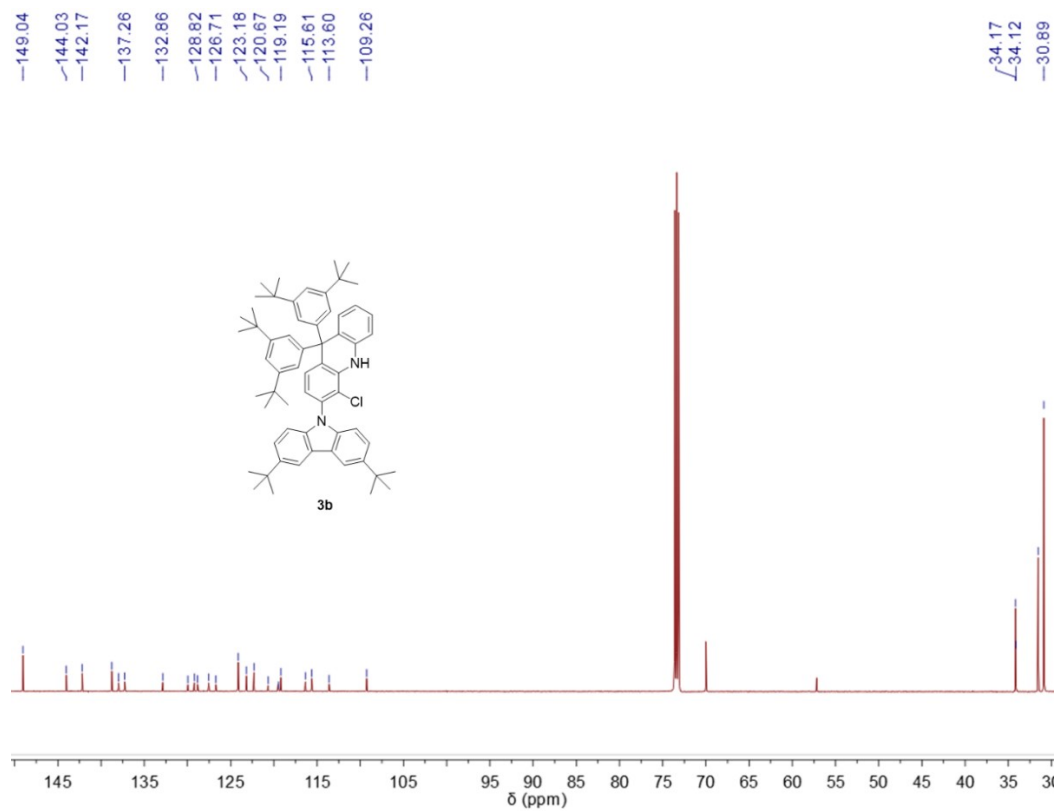
Figure S20. ^{13}C NMR spectra of **3b**.

Figure S21. ^1H NMR spectra of **4a.**

Figure S22. ^{13}C NMR spectra of **4a.**
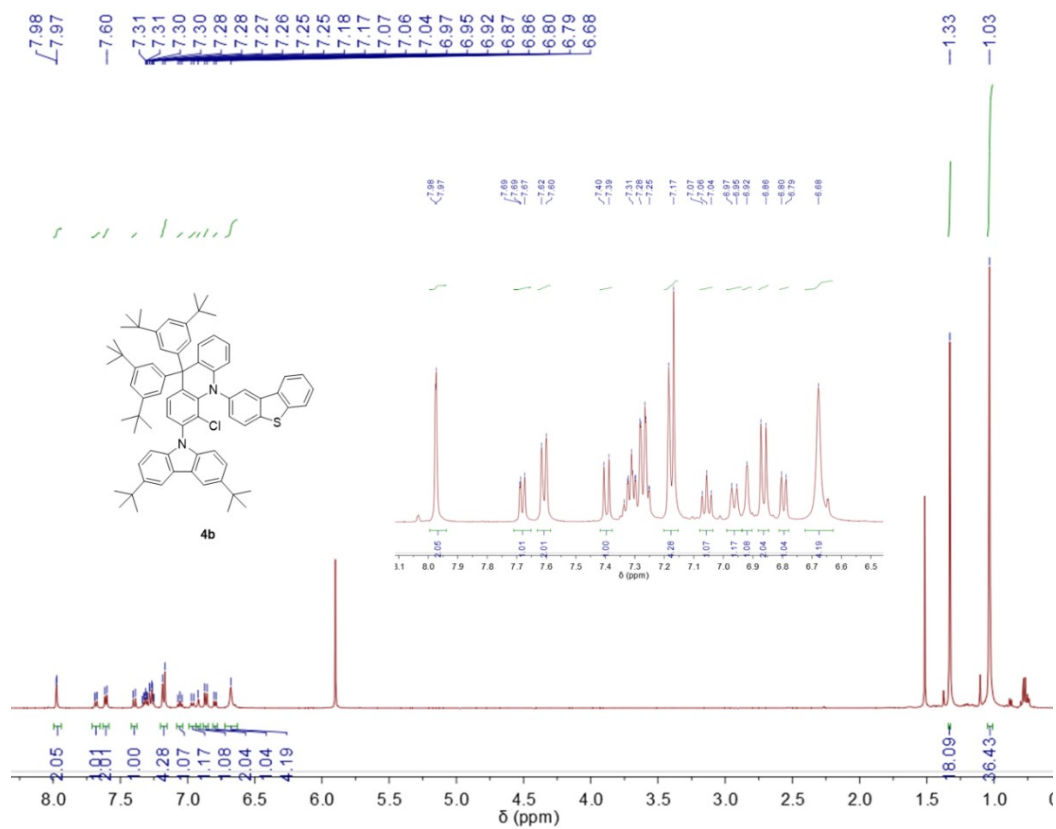
Figure S23. ^{1}H NMR spectra of **4b.**
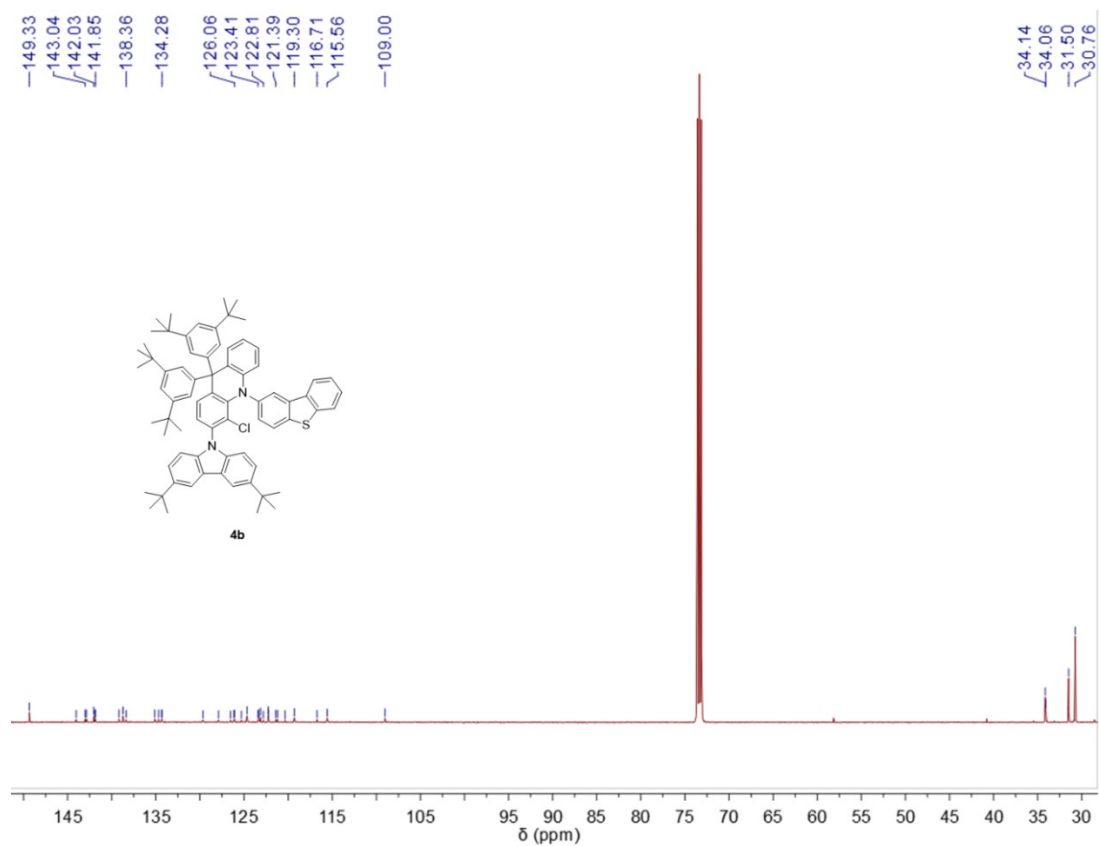
Figure S24. ^{13}C NMR spectra of **4b.**
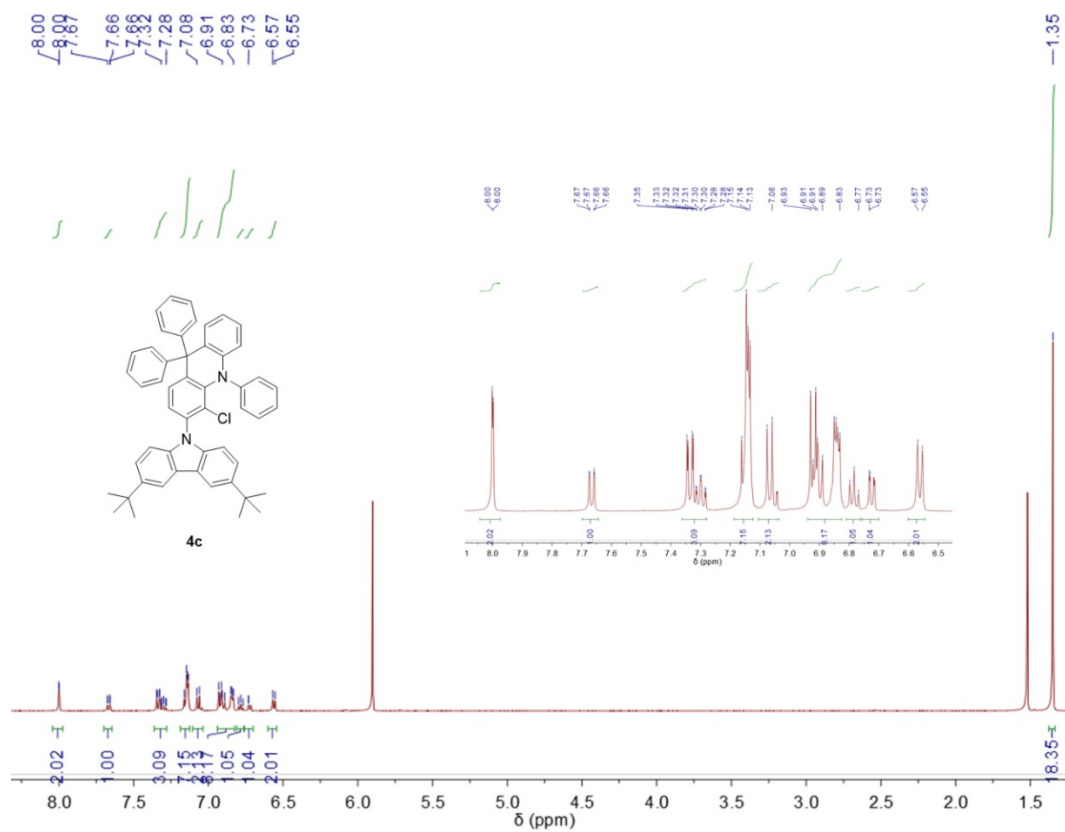
Figure S25. ^{1}H NMR spectra of **4C.**
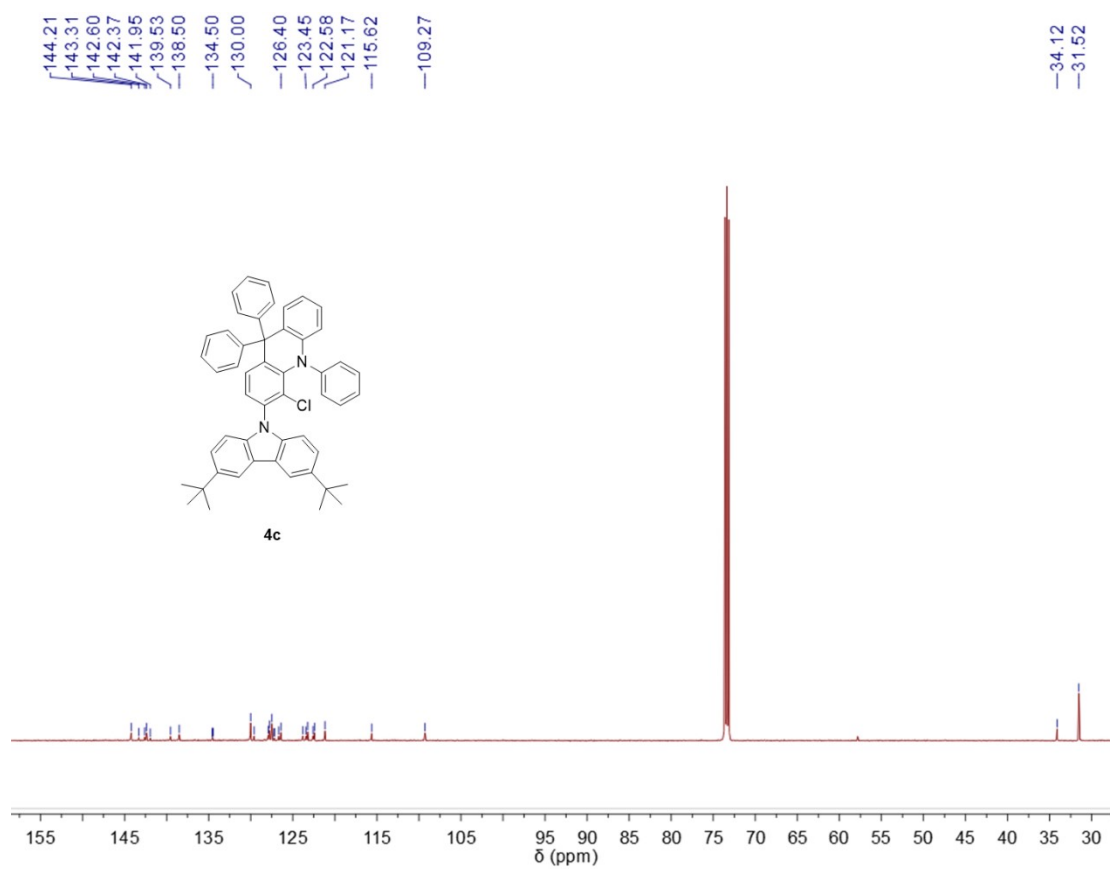
Figure S26. ^{13}C NMR spectra of **4C.**
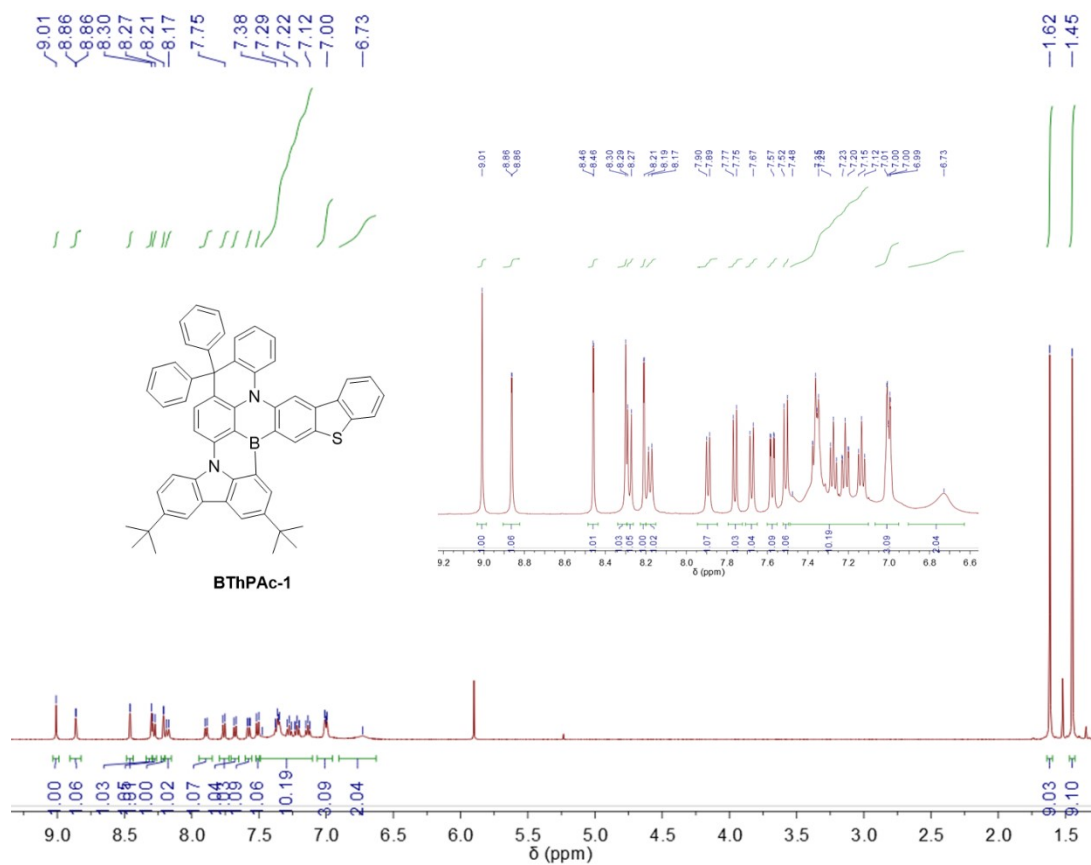
Figure S27. ¹H NMR spectra of **BThPAc-1.**
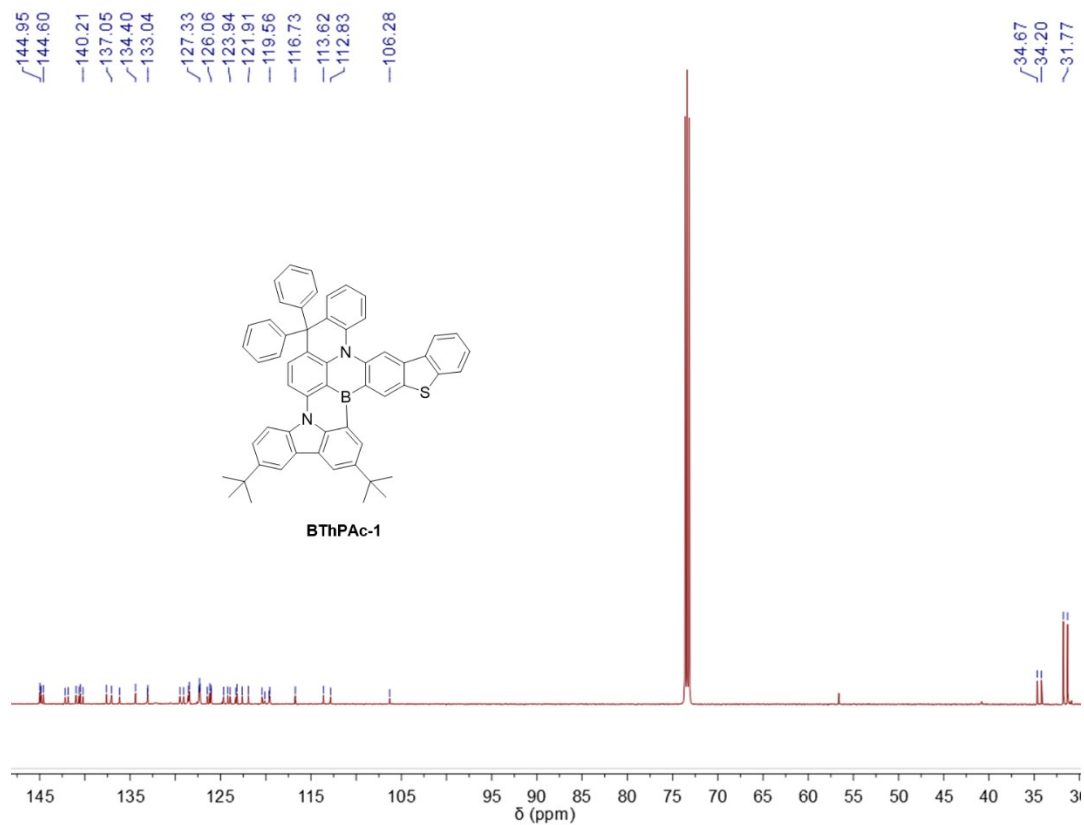
Figure S28. ¹³C NMR spectra of **BThPAc-1.**

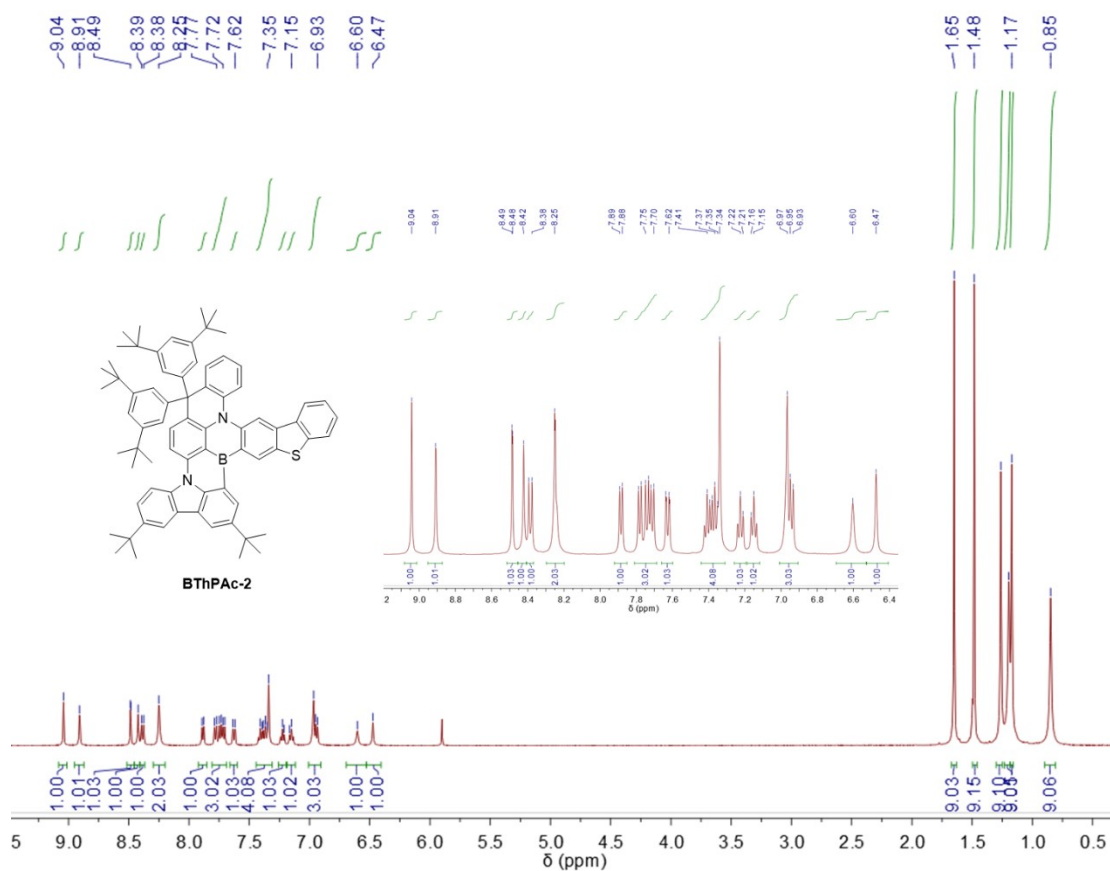**Figure S29**. MALDI-TOF of **BThPAc-1.**

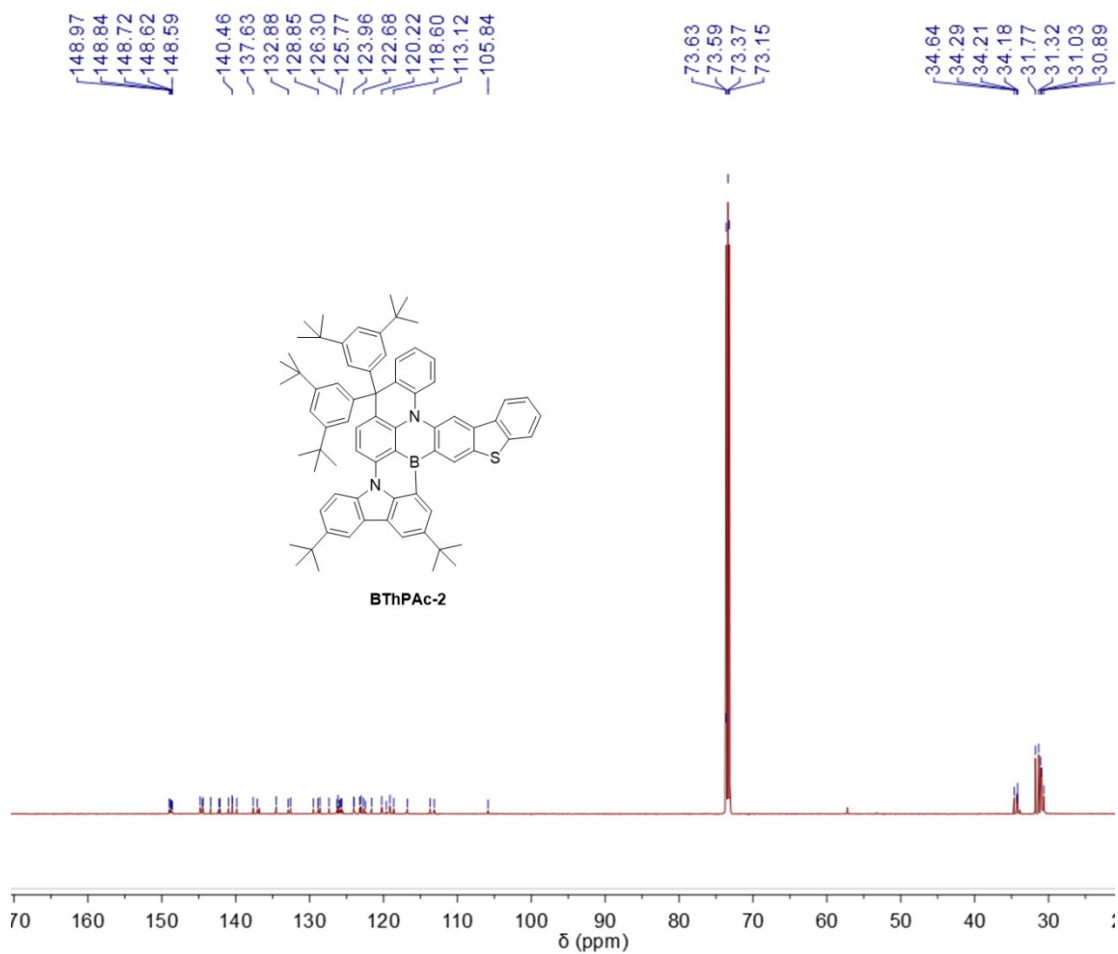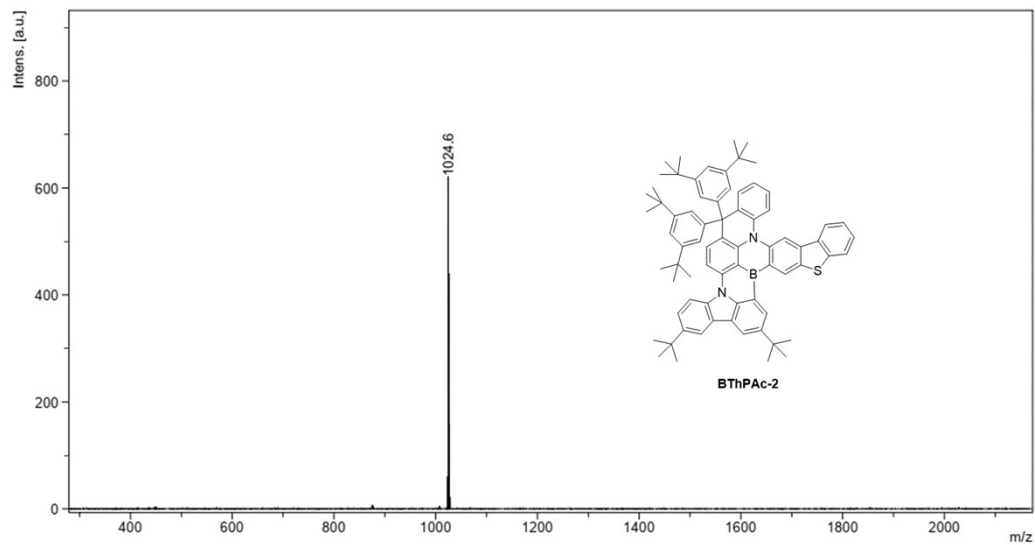**Figure S30**. ^{1}H NMR spectra of **BThPAc-2.**
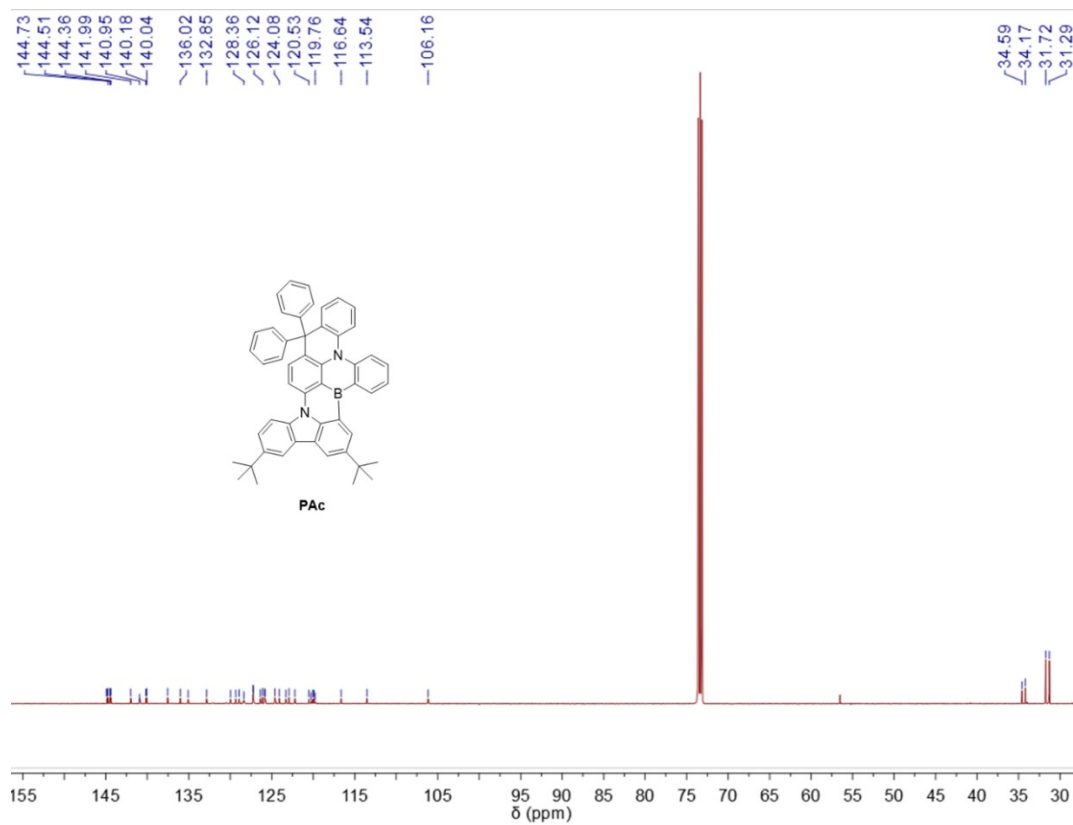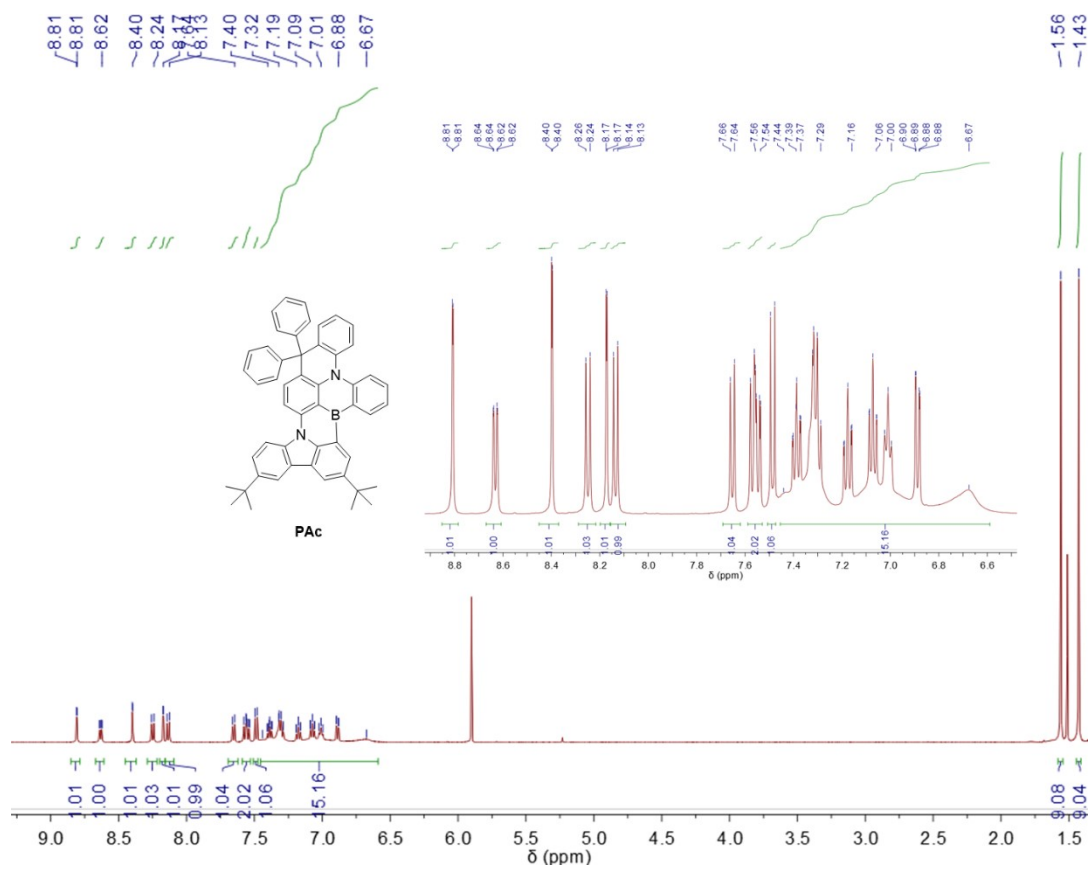
Figure S31. ^{13}C NMR spectra of **BThPAc-2.**

D:\Data\2023\0512\ms230511-11-zr-t\0_K19\1

Comment 1
Comment 2

Bruker Daltonics flexAnalysis

Figure S32. MALDI-TOF of **BThPAc-2.**

Figure S33. ^{1}H NMR spectra of **PAc.**

Figure S34. ^{13}C NMR spectra of **PAc.**

10.Supporting Imformation References

S1   Gaussian 09, Revision C.01, Frisch, M. J.; Trucks, G. W.; Schlegel, H. B.; Scuseria, G. E.; Robb, M. A.; Cheeseman, J. R.; Scalmani, G.; Barone, V.; Mennucci, B.; Petersson, G. A.; Nakatsuji, H.; Caricato, M.; Li, X.; Hratchian, H. P.; Izmaylov, A. F.; Bloino, J.; Zheng, G.; Sonnenberg, J. L.; Hada, M.; Ehara, M.; Toyota, K.; Fukuda, R.; Hasegawa, J.; Ishida, M.; Nakajima, T.; Honda, Y.; Kitao, O.; Nakai, H.; Vreven, T.; Montgomery, Jr., J. A.; Peralta, J. E.; Ogliaro, F.; Bearpark, M.; Heyd, J. J.; Brothers, E.; Kudin, K. N.; Staroverov, V. N.; Keith, R.; Kobayashi, R.; Normand, J.; Raghavachari, K.; Rendell, A.; Burant, J. C.; Iyengar, S. S.; Tomasi, J.; Cossi, M.; Rega, N.; Millam, N. J.; Klene, M.; Knox, J. E.; Cross, J. B.; Bakken, V.; Adamo, C.; Jaramillo, J.; Gomperts, R.; Stratmann, R. E.; Yazyev, O.; Austin, A. J.; Cammi, R.; Pomelli, C.; Ochterski, J. W.; Martin, R. L.; Morokuma, K.; Zakrzewski, V. G.; Voth, G. A.; Salvador, P.; Dannenberg, J. J.; Dapprich, S.; Daniels, A. D.; Farkas, Ö.; Foresman, J. B.; Ortiz, J. V.; Cioslowski, J.; Fox, D. J. Gaussian, Inc., Wallingford CT, 2010., accessed.

S2   F. Weigend, *Phys. Chem. Chem. Phys.* 2006, **8**, 1057.

S3   F. Neese, *WIREs Comput. Mol. Sci.* 2017, **8**, e1327.

S4   M. Kallay, P. R. Nagy, D. Mester, Z. Rolik, G. Samu, J. Csontos, J. Csoka, P. B. Szabo, L. Gyevi-Nagy, B. Hegely, I. Ladjanszki, L. Szegedy, B. Ladoczki, K. Petrov, M. Farkas, P. D. Mezei, A. Ganyecz, *J. Chem. Phys.* 2020, **152**, 074107.

S5   "MRCC, a quantum chemical program suite written by M. Kállay, P. R. Nagy, D. Mester, L. Gyevi-Nagy, J. Csóka, P. B. Szabó, Z. Rolik, G. Samu, J. Csontos, B. Hégely, Á. Ganyecz, I. Ladjánszki, L. Szegedy, B. Ladóczki, K. Petrov, M. Farkas, P. D. Mezei, and R. A. Horváth. See www.mrcc.hu.", accessed.

S6   T. Lu, F. Chen, *J. Comput. Chem.* 2012, **33**, 580.

S7   W. Humphrey, Dalke, A. and Schulten, K., *J. Molec. Graphics* 1996, **14.1**, 33.

S8   N. Ikeda, S. Oda, R. Matsumoto, M. Yoshioka, D. Fukushima, K. Yoshiura, N. Yasuda, T.Hatakeyama, *Adv. Mater.* 2020, **32**, 2004072

S9   Y. Zhang, J. Wei, D. Zhang, C. Yin, G. Li, Z. Liu, X. Jia, J. Qiao, L. Duan, *Angew. Chem. Int. Ed.* 2022, **61**, e202113206.

S10 P. Jiang, J. Miao, X. Cao, H. Xia, K. Pan, T. Hua, X. Lv, Z. Huang, Y. Zou, C. Yang, *Adv. Mater.* 2022, **34**, 2106954.

S11 Y. Xu, C. Li, Z. Li, Q. Wang, X. Cai, J. Wei, Y. Wang, *Angew. Chem. Int. Ed.* 2020, **59**, 17442.

S12 H. J. Cheon, S. J. Woo, S. H. Baek, J. H. Lee, Y. H. Kim, *Adv. Mater.* 2022, **34**, 2207416.

S13 J. Bian, S. Chen, L. Qiu, R. Tian, Y. Man, Y. Wang, S. Chen, J. Zhang, C. Duan, C. Han, H. Xu, *Adv. Mater.* 2022, **34**, 2110547.

S14 Y. N. Hu, X. C. Fan, F. Huang, Y. Z. Shi, H. Wang, Y. C. Cheng, M. Y. Chen, K. Wang, J. Yu, X. H. Zhang, *Adv. Opt. Mater.* 2022, **11**, 2202267.

S15 F. Huang, X. C. Fan, Y. C. Cheng, H. Wu, Y. Z. Shi, J. Yu, K. Wang, C. S. Lee, X. H. Zhang, *Mater. Horiz.* 2022, **9**, 2226.

S16 X. F. Luo, H. X. Ni, X. Liang, D. Yang, D. Ma, Y. X. Zheng, J. L. Zuo, *Adv. Opt. Mater.* 2023, **11**, 2203002.

S17 Y. Chang, Y. Wu, K. Zhang, S. Wang, X. Wang, S. Shao, L. Wang, *Dyes and Pigments* 2023, **220**, 111678.

S18 N. Peethani, N. Y. Kwon, C. W. Koh, S. H. Park, J. M. Ha, M. J. Cho, H. Y. Woo, S. Park, D. H. Choi, *Adv. Opt. Mater.* 2023, **12**, 2301217.